Title
Statistical models for longitudinal analysis of single and mixed species infections

Author
Colborn, Kathryn Louise

Publication Date
2013

Peer reviewed|Thesis/dissertation

Statistical models for longitudinal analysis of single and mixed species infections

By
Kathryn Louise Colborn

A dissertation submitted in partial satisfaction of the
requirements for the degree of
Doctor of Philosophy
in
Biostatistics
in the
Graduate Division
of the
University of California, Berkeley

Committee in charge:
Professor Terence P. Speed, Chair
Professor Sandrine Dudoit
Professor Lisa Barcellos

Fall 2013

Statistical models for longitudinal analysis of single and mixed species infections

Abstract
Statistical models for longitudinal analysis of single and mixed species infections
By
Kathryn Louise Colborn
Doctor of Philosophy in Biostatistics
University of California, Berkeley
Professor Terence P. Speed, Chair

There are numerous examples of infectious diseases that are caused by various species of the same pathogen. Some examples include Lyme disease, malaria, Leishmaniasis, Dengue fever, and Ehrlichiosis. The advancement of laboratory methods has facilitated more sensitive detection of mixed species infections in humans, which has resulted in a surge of research focussing on the effects of mixed infections on clinical outcomes. Cross-sectional blood samples compared with clinical outcome measures provide a limited scope of the interactions between species. It is important to study these infections in humans longitudinally, and within their natural environments, in order to develop an understanding of the complex relationships between hosts, pathogens and vectors of transmission.

Papua New Guinea is a country with high prevalence of both *Plasmodium falciparum* and *P. vivax*, two species of parasites that can cause malaria. It is well known that these two parasites can cause severe morbidity and mortality independently, but there has not been conclusive evidence of the effect of mixed *P. falciparum* and *P. vivax* infections on clinical symptoms. Children under age five are at highest risk of experiencing adverse outcomes from *Plasmodium* infections. In 2006, a cohort study was implemented to conduct an investigation of the effects of mixed *P. falciparum* and *P. vivax* infections on clinical episodes of malaria in children living in a rural area of Papua New Guinea. The data collected from this study are used throughout this dissertation to address both the epidemiological questions of the study investigators and to present statistical models for analyzing longitudinal malaria data and mixed species infections.

Contents

List of Tables

List of Figures

1 Introduction

Malaria is an infectious disease caused by *Plasmodium* parasites transmitted by female *Anopheles* mosquitoes. The five species of *Plasmodium* that infect humans are *P. falciparum*, *P. vivax*, *P. malaria*, *P. ovale* and *P. knowlesi*. The majority of deaths due to malaria worldwide are among children and pregnant women and are caused by either *P. falciparum* (*Pf*) or *P. vivax* (*Pv*). The disease is classified as either uncomplicated or complicated. Uncomplicated malaria is characterized by fever, chills and flu-like symptoms. Complicated malaria can include serious organ failures and severe anemia.

The malaria parasite has two hosts: humans and mosquitoes. When feeding on a human, an infected female *Anopheles* mosquito can inoculate sporozoites into a human's bloodstream. These sporozoites then enter liver cells and mature into schizonts. The schizonts then rupture the liver cells releasing merozoites, which infect red blood cells. It is the merozoite stage when individuals experience symptoms of malaria. Some merozoites differentiate into gametocytes, which when ingested by a mosquito taking a bloodmeal, can develop into sporozoites in the mosquito, thus completing the life cycle. The typical incubation period for onset of symptoms for *Pf* malaria is one to three weeks. *Pv* malaria symptoms can present within three weeks of a bite by an infective mosquito; however, the liver stages can remain dormant for up to four years.

Papua New Guinea (PNG) is an Australasian country in the South Pacific with endemic transmission of *Pf* and *Pv* malaria. It has a tropical climate with distinct rainy and dry seasons. The majority of its population live in rural villages and engage in subsistence agriculture. Malaria in PNG is unique because *Pv* is the predominant species in children less than three years of age, yet there are high rates of *Pf* in all age groups. For this reason, PNG was selected as the site of a longitudinal cohort study to investigate the utility of biological markers for predicting *Pf* and *Pv* malaria episodes and to measure the effect of mixed infections of these two species on malaria symptoms. A cohort of 264 children from 11 villages in PNG and aged one to three years at study enrollment were actively followed for 16 months. Each child was visited every eight weeks to ascertain behavioral information and to obtain blood samples. All blood samples were genotyped, and positive samples were classified by species. Children were also visited every two weeks to determine whether they were experiencing symptoms of malaria. If a child was febrile, a blood sample was taken and a diagnosis of malaria was determined. Each confirmed case of malaria was recorded at two weeks visits, eight weeks visits and intermittent visits to the area health clinics. Each child with confirmed malaria was treated with either artemether-lumefantrine or amodiaquine plus sulphadoxine-pyramethamine. Details of this study have been described previously (Lin et al., 2010).

This thesis describes statistical models for addressing the epidemiological questions of the PNG cohort study investigators. In Chapter 2 we implement generalized linear mixed models to estimate the effect of a biological measure of exposure to infective mosquito bites on subsequent single-species clinical episodes of malaria caused by *Pf* or *Pv* parasites, separately. In Chapter 3, we describe a bivariate statistical model for estimating association between the ex-

posure variables for the two species. Chapter 4 presents analyses of the effects of mixed species infections on clinical outcomes. We summarize our conclusions in Chapter 5.

I carried out the statistical analyses described for each of the chapters in this thesis. The *Pf* results presented in Chapter 2 have been published, and the *Pv* results from Chapter 2 will be published soon. The contents of Chapter 2 have been adapted from the published manuscripts and include more of the statistical methods.

2 Longitudinal analysis of single-species infections and clinical episodes

The PNG study was a longitudinal cohort with a repeated measures design. Each child contributed up to eight observations, each of which were separated by eight weeks of time. The nature of this study design warranted statistical methods that would permit us to account for correlation among repeated observations from the same child and correlation among observations from children residing in the same village. We chose to use random effects models because they permit inclusion of more than one level of correlation. In previous analyses of these data, marginal models were used to account for repeated measures from the same child; however, village of residence was specified as an 11 category fixed effect. This specification required 10 degrees of freedom for the village effect. The random effects model used only one degree of freedom for village by specifying it as a random, or clustering, effect. None of the response variables of interest were normally distributed but were from the exponential family of distributions. Therefore, we used generalized linear mixed models (GLMMs) to relate the explanatory variables and individual and village-specific random effects to the outcomes of interest (Diggle et al., 2002).

We describe the GLMM in detail in the next section. The remainder of this chapter will focus on longitudinal analysis of single-species infections and clinical episodes from the PNG cohort. GLMMs will be used to model the primary research outcomes from the study.

2.1 Generalized linear mixed models

A generalized linear model (GLM) is a linear model that can be generalized to a response that is not normally distributed. A GLM uses a link function to relate the linear predictor (i.e. fixed effects) to the mean of the distribution of the response (McCullagh and Nelder, 1989). A GLMM is an extension of a GLM that includes normally distributed random effect(s) in the linear predictor.

One of the primary outcomes of interest in the PNG study was the number of clinical episodes experienced during an eight weeks interval. Let $i = 1, \ldots, n$ represent the n villages, let $j = 1, \ldots, n_i$ denote the n_i children within a village i, and let $k = 1, \ldots, n_{ij}$ indicate the kth observation for child j from village i. Denote the responses, $Y_{ij1}, \ldots, Y_{ijn_{ij}}$, counts of clinical episodes between an eight weeks period, which were assumed to be mutually independent observations from a Poisson distribution, conditional on a child nested within a village. The Poisson GLMM can be expressed by the following

$$\log\{E(Y_{ijk}|\nu_i, c_{ij})\} = \boldsymbol{x}'_{ijk}\boldsymbol{\beta} + \nu_i + c_{ij}, \tag{2.1}$$

where $\boldsymbol{x}$ is a matrix of fixed effects, $\boldsymbol{\beta}$ is a vector of fixed effect coefficients and $\nu_i \sim N(0, \sigma^2_\nu)$

and $c_{ij} \sim N(0, \sigma_c^2)$ represent the random effects of villages and children, respectively. The log function is the canonical link of the Poisson distribution. Other link functions and response distributions will be introduced later in this chapter. The exponentiated coefficients from the Poisson GLMM model are interpreted as relative risks. Furthermore, GLMMs produce subject-specific parameter estimates. Therefore, a fixed effect coefficient from this model represents the excess risk of experiencing the outcome given a one unit increase in the fixed effect for a given child.

Covariates for each model were selected based on earlier analyses of the same data (Lin et al., 2010). Exploratory data analysis guided the specification of the model when the relationships between the covariates and the outcome did not appear to be linear, such as with age, $_{mol}$FOI annualized rate and season. Seasonality was characterized by two readily interpretable parameters - amplitude and phase - which defined non-linear regression terms. For computational convenience, they were replaced by fixed phase sine and cosine terms (Diggle et al., 2002). We set the period, T, of the sine and cosine functions to be 52 weeks, or approximately one year, and the start of the function at week one. Thus, the following formula was included in the GLMMs,

$$f(w) = \beta_1 \sin\Big(\frac{2\pi w}{52}\Big) + \beta_2 \cos\Big(\frac{2\pi w}{52}\Big), \tag{2.2}$$

where w was the week of the year (e.g. $w = 1$ was the first week of January and $w = 52$ was the last week of December), β_1 was the coefficient for the sine function and β_2 was the coefficient for the cosine function. The amplitude, α, was calculated by the following

$$\alpha = \sqrt{\beta_1^2 + \beta_2^2}. \tag{2.3}$$

The two extreme values of the function were found by solving

$$w = \arctan\Big(\frac{\beta_1}{\beta_2}\Big)\frac{52}{2\pi}. \tag{2.4}$$

If $\beta_1/\beta_2 > 0$, then the w obtained from (2.4) was the first extreme and the second was $w + 26$. If $\beta_1/\beta_2 \leq 0$, then the two extremes were $w + 26$ and $w + 52$. If $\beta_1 > 0$, then the first extreme was a peak, and if $\beta_1 \leq 0$, then the first extreme was the trough.

For all outcomes that were affected by residual treatment duration, an offset was fit to adjust for years-at-risk during each interval. Estimation of these models was done using the LME4 package (Bates et al., 2012) in R version 2.12 (R Core Team, 2013).

2.2 Objectives of single-species analyses

The objectives of the analyses presented in this chapter were to estimate the relationships between important individual and environmental exposures and prevalence and incidence of clinical malaria caused by *Pf* and *Pv* parasites, separately. Transmission intensity is traditionally quantified through entomological measures of exposure, in particular the entomological inoculation rate (EIR) (Hay et al., 2000). However, accurately measuring EIRs is notoriously difficult and labor intensive (Dye, 1992). The force of infection (FOI), defined as the number of *Plasmodium* infections acquired over time, has long been proposed as an alternative mea-

sure of transmission intensity, and different approaches to measuring FOI have been proposed. For example, infant conversion rate (Macdonald, 1950) (i.e. time to a patent infection in uninfected children less than one year of age) was widely used in the 1950-70s, and while being an excellent marker for transmission intensity, it required monitoring of a large number of very young children over long periods. An alternative method of estimating the FOI of *Plasmodium* species is microscopical detection of parasites following antimalarial treatment. This method has been applied in field trials of vector control and vaccines (Msuya and Curtis, 1991; Alonso et al., 2004). This study intended to use $_{mol}$FOI as a cheaper, more easily acquired measurement of exposure to infective mosquito bites than the methods described above. Furthermore, the objective was to estimate the magnitude of the effect of this variable on predicting malaria clinical episodes.

Polymerase chain reaction (PCR) methods provide greater sensitivity for detecting clones (i.e. unique genetic sequences) than light microscopy (LM) because they permit genotyping individual parasite infections (Smith et al., 1999; Smith and Vounatsou, 2003; Sama et al., 2006; Falk et al., 2006). In the PNG study, molecularly determined FOI ($_{mol}$FOI) was estimated by genotyping longitudinal blood samples and comparing the newly acquired clones over a period of time to those from previous blood samples. A second molecular parameter, multiplicity of infection (MOI), was also generated by genotyping cross-sectional blood samples. MOI is defined as the number of unique *Plasmodium* genotypes in a cross-sectional blood sample. It differs from $_{mol}$FOI in that it cannot differentiate between long-lasting infections and new infections.

The primary objectives of the analyses presented in this chapter were to determine the effects of important individual and environmental covariates on prevalence of infections and incidence of malaria and to determine the magnitude of effect of $_{mol}$FOI on the rate of clinical malaria episodes experienced over a period of time. Section 2.4 describes the analyses and results for *Pf* infections and clinical episodes, and Section 2.5 presents the analyses and results for *Pv*.

2.3 Description of cohort

Of the 264 children recruited for the study, 94% were retained until the end of the study, with between 96.0% - 100.0% of children seen at each scheduled eight weeks blood sampling. Children were between 0.9 to 3.2 years of age at study enrollment (median 1.7, interquartile range (IQR): [1.3, 2.4]). A summary of participants' characteristics and biological measurements is provided in Table 2.1. The next two sections present results from fitting GLMMs to single-species prevalence, MOI, $_{mol}$FOI and clinical episodes of malaria caused by either *Pf* or *Pv* parasites.

2.4 Analysis of *Pf* infections and clinical episodes

Pf positive blood samples were determined by extracting DNA from cell pellets using QIAamp 96 DNA Blood Kits (Qiagen, Australia) according to the manufacturer's instructions. All samples were genotyped for the marker gene merozoite surface protein 2 (msp2) by use of capillary electrophoresis for fragment sizing, as previously described by Falk et al. (2006), with some minor changes and adaptations of PCR conditions for highly purified DNA as described by Schoepflin et al. (2009). The msp2 marker was highly polymorphic in the study area, with a total of 52 different msp2 genotypes identified (Schoepflin et al., 2009). Clinical episodes attributed to *Pf* parasites were defined as light microscopically detected parasitemia greater than 2500 parasites per μl and a body temperature greater than 37.5 degrees Celsius.

Table 2.1: Characteristics of study participants and biological measurements from 8 weeks interval visits.

Total number of study participants	264
Total number of 8 weeks interval visits	1,865
Average age at study enrollment (sd)	1.84 (0.66)
Median proportion of intervals slept under an ITN (IQR)	0.22 (0, 1)
Total (%)* *Pf* infections at interval visits	
PCR	744 (40)
LM	531 (28)
Total (%)* *Pv* infections at interval visits	
PCR	1,135 (61)
LM	965 (52)
Incidence rates per person-years-at-risk (95% CI)†	
Pf clinical episodes	1.9 (1.75, 2.11)
Pv clinical episodes	1.6 (1.44, 1.76)
Pf $_{mol}$FOI	5.4 (5.11, 5.79)
Pv $_{mol}$FOI	15.3 (14.08, 15.96)

*Percent of all 8 weeks visits; †Per person-years-at-risk over entire cohort, confidence intervals (CI) from Haenszel et al. (Haenszel et al., 1962).

2.4.1 *Pf* prevalence and MOI

Eighty-seven percent of children had *Pf* infections detected by PCR at least once during the study period. Prevalence of infection was significantly positively associated with age (at start of interval, Table 2.2, odds ratio (OR) 5.50), ranging from an average of 25% for children aged 12 months, to 49% for children aged 24 to 30 months (Figure 2.1, column 1, row 1). The effect of age on prevalence leveled off after a child became 2.5 years of age (Figure 2.1, column1, row 1; Table 2.2 age^2 OR 0.77). Consistent with previous findings (Lin et al., 2010), recent treatment with antimalarials and the presence of a febrile illness were both associated with increased risk of *Pf* infection (Table 2.2, Prevalence). Despite adjusting for these factors, prevalence of infection still varied significantly between villages and between children within villages (Table 2.2, Prevalence, random effects). Prevalence also showed strong seasonal variation (Table 2.2; Figure 2.1, column 1, row 2), ranging from a low average of 31% in early August to a high of 52% in early February. Use of an insecticide treated bed net (ITN) was associated with a very strong reduction in *Pf* prevalence (Table 2.2 OR 0.36; Figure 2.1, column 1, row 3), dropping from an average of 56% with no ITN use to 22% when an ITN was always used.

Unlike prevalence of infection, MOI continued to increase significantly throughout the age range (Table 2.2; Figure 2.1, column 2, row 1), from about 1.3 clones at one year of age to 2.2 clones at four years of age. Average ITN use was also associated with a reduction in MOI (Table 2.2; Figure 2.1, column 2, row 3). MOI was not affected by seasonal variation (Figure 2.1, column 2, row 2) and there was no significant variation in MOI between and within villages (Table 2.2, random effects).

2.4.2 *Pf* $_{mol}$FOI

Excluding any period with residual drug levels from the time at risk (two to four weeks, depending on the medication), the $_{mol}$FOI annualized rate was 5.4 new *Pf* infections per child

Figure 2.1: Exploratory plots using smooth splines for age, season and ITN use by prevalence, MOI, $_{mol}$FOI and incidence of *Pf* malaria.

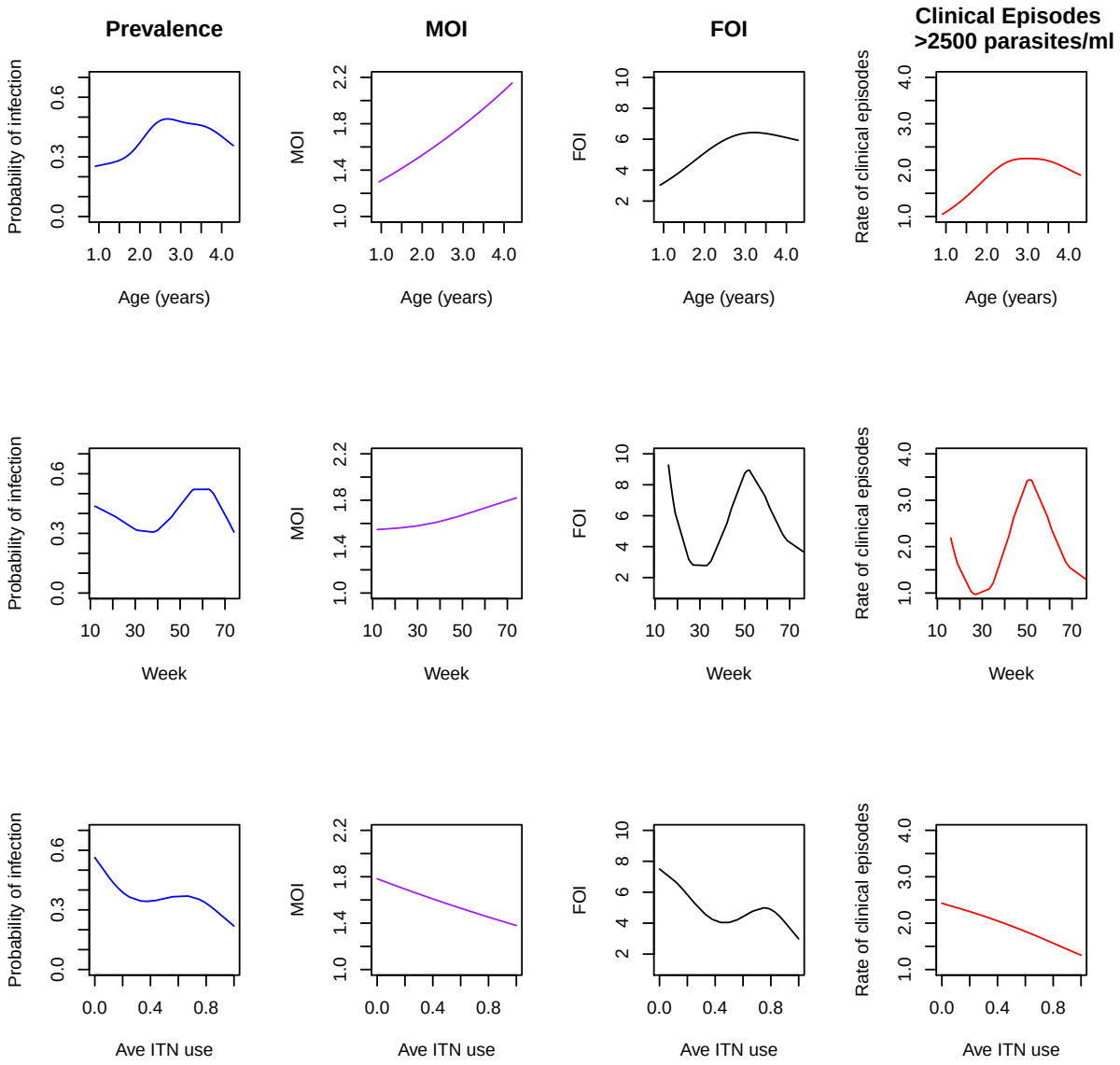

per year. The GLMM model for $_{mol}$FOI was fit with an offset to account for the time under residual drug effects. $_{mol}$FOI showed a very pronounced seasonality (Table 2.2, incidence rate ratio (IRR) sin(weeks) 1.53, IRR cos(weeks) 1.56), ranging from a peak of 9.3 clones per year in early February to a low of 2.8 clones per year at the beginning of August (Figure 2.1, column 3, row 2). ITN use was associated with a significant reduction (Table 2.2, IRR 0.49) in acquisition of new clones from a high of 7.5 clones per year with no ITN usage to a low of 3.0 clones per year with regular use (Figure 2.1, column 3, row 3). $_{mol}$FOI appeared to increase linearly between one and three years of age with little difference thereafter (Figure 2.1, column 3, row 1); however, the quadratic term was not significant. There was significant variation in $_{mol}$FOI both between villages and between children living in the same village (Table 2.2, $_{mol}$FOI random effects).

Table 2.2: Parameter estimates from GLMMs for *Pf* prevalence, MOI and $_{mol}$FOI (95% confidence intervals, CI).

	Prevalence			**MOI**			$_{mol}$**FOI**		
	OR	**95% CI**	**p value**	**OR**	**95% CI**	**p value**	**IRR**	**95% CI**	**p value**
Fixed effects									
Age (at interval)	5.50	[2.10, 14.4]	0.0005	1.17	[1.08, 1.27]	<0.001	1.38	[1.23, 1.56]	<0.001
Age^2	0.77	[0.64, 0.93]	0.006						
Season									
Sin (week)	1.37	[1.17, 1.59]	<0.001				1.53	[1.37, 1.70]	<0.001
Cos (week)	1.42	[1.21, 1.67]	<0.001				1.56	[1.46, 1.71]	<0.001
Year (2007)							0.49	[0.42, 0.59]	<0.001
ITN use	0.36	[0.24, 0.54]	<0.001	0.77	[0.67, 0.89]	0.0003	0.49	[0.38, 0.61]	<0.001
Treated 28 days	2.17	[1.70, 2.76]	<0.001						
Fever	1.62	[1.22, 2.16]	0.001				1.22	[1.06, 1.39]	0.004
Random effects	**Variance**			**Variance**			**Variance**		
Village	0.38		<0.001	~0		0.5	0.05		0.001
Child	0.43		<0.001	~0		0.5	0.22		<0.001
Seasonal effects									
Amplitude	0.47						0.62		
Peak(week)	6						6		
Trough (week)	32						32		

2.4.3 Clinical episodes of malaria caused by *Pf* parasites

A total of 1,134 febrile episodes (incidence rate (IR) 4.60 per child per year) with parasitemia (determined by light microscopy) were observed over the 16 months of followup. *Pf* was the most common cause of malarial illness (any density: IR 2.6 per child per year; *Pf* > 2500 parasites/μl: IR 1.9 per child per year) followed by *Pv* (any density: IR 2.5 per child per year; Pv > 500 parasites/μl: IR 1.6 per child per year). *P. malariae* and *P. ovale* episodes were rare. All further analyses were done using only the more specific definition of *Pf* malaria, defined as febrile illness plus *Pf* parasitemia > 2500 parasites/μl. The GLMMs in Table 2.3 were fit using an offset, again, to adjust for the time under residual drug effects.

Age (at interval), season, ITN use and recent antimalarial treatment were all significant predictors of clinical episodes of *Pf* malaria (Table 2.3, model excluding $_{mol}$FOI). The incidence of *Pf* malaria peaked at 3.4 clinical episodes per child per year early in the rainy season (early January), and was lowest at 1.0 per child per year in the middle of the dry season (early July, Figure 1B). The incidence of *P. falciparum* malaria increased non-linearly with age (Figure 2.1, column 4, row 2). Children three years of age experienced 2.3 clinical episodes per year on average and children one year of age experienced only 1.0 clinical episode per year (Figure 2.1, column 4, row 1). ITN use appeared to be protective against clinical episodes, where children that did not use and ITN experienced 2.4 episodes per year compared to only 1.3 episodes per year in children that used an ITN regularly (Table 2.3 IRR 0.59; Figure 2.1, column 4, row 3). Interestingly, even after adjusting for all of the above factors, the incidence of *Pf* malaria still varied significantly between villages and between children within villages (Table 2.3, model excluding $_{mol}$FOI random effects).

An important contribution to the analyses presented in this section was the addition of $_{mol}$FOI to the model predicting clinical episodes (Table 2.3). Again, this variable was considered to be the most important factor for measuring malaria transmission in the region of the study. $_{mol}$FOI was also affected by residual drug treatment effects, as we discussed in the previous analysis; therefore, we divided it by the years-at-risk to create the rate of acquisition of new clones. However, this variable was highly positively skewed. We tried various transformations, and the one that yielded the lowest log-likelihood when fit to the GLMM was a cube root transformation. This variable was used in the model described in Table 2.3. When $_{mol}$FOI was added to the model, it was strongly positively associated with an increase in the incidence of malaria (Table 2.3, IRR 2.12). Adjusting for $_{mol}$FOI reduced the influence of all other factors previously associated with incidence of *Pf* malaria (comparing the two models in Table 2.3). ITN use, age and recent antimalarial treatment were no longer significantly associated with incidence of *Pf* malaria once $_{mol}$FOI was added to the model. Similarly, the variability between villages and between children within a village were no longer significant (Table 2.3, model including $_{mol}$FOI random effects). Although significant seasonal variation in incidence remained, adjustment for $_{mol}$FOI halved the range of the seasonal variation and shifted the peak of incidence by six weeks (Table 2.3, Amplitude; Figure 2.2). Consequently, after taking into account the rate of clone acquisition during an interval, the risk of experiencing clinical *Pf* illness was highest at the beginning of the rainy season (i.e. week 48) and lowest at the start of the dry season (week 22). $_{mol}$FOI was the most important factor associated with the rate of clinical episodes caused by *Pf* measured in this study. Analyses for febrile illness with concurrent parasitemia with any density yielded comparable results (not shown).

Table 2.3: Parameter estimates from GLMMs for clinical episodes caused by *Pf* parasites.

	Model excluding $_{mol}$FOI			**Model including $_{mol}$FOI**		
	IRR	**95% CI**	**p value**	**IRR**	**95% CI**	**p value**
Fixed effects						
Age (at interval)	3.34	[1.35, 8.27]	0.009	1.60	[0.69, 3.71]	0.3
Age^2	0.83	[0.69, 0.98]	0.03	0.92	[0.78, 1.08]	0.3
Season						
Sin (week)	1.13	[0.94, 1.34]	<0.001	0.89	[0.74, 1.07]	<0.001
Cos (week)	1.69	[1.48, 1.93]	<0.001	1.29	[1.13, 1.47]	< 0.001
Year (2007)	0.73	[0.55, 0.96]	0.03	1.09	[0.83, 1.44]	0.5
ITN use	0.59	[0.44, 0.79]	<0.001	0.93	[0.73, 1.18]	0.6
$(_{mol}FOI)^{1/3}$				2.12	[1.93, 2.31]	<0.001
Random effects	**Variance**			**Variance**		
Village	0.06		0.005	0.01		0.2
Child	0.16		0.005	<0.001		0.5
Seasonal effects						
Amplitude	0.54			0.28		
Peak(week)	2			48		
Trough (week)	28			22		

Figure 2.2: Incidence rate ratios for age (1 year of age reference) and season (first week of the year reference) by incidence of *Pf* malaria, before (blue) and after (red) adjusting for $_{mol}$FOI.

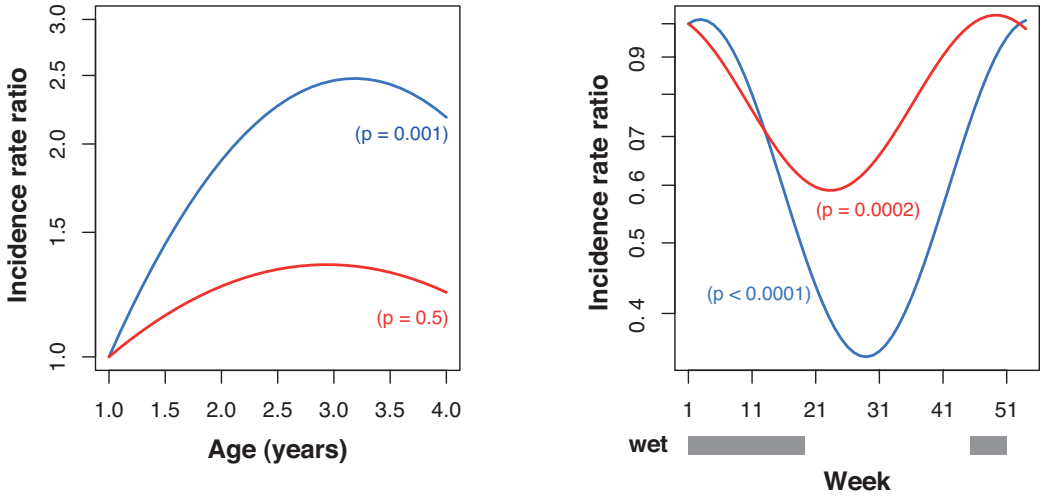

2.4.4 Discussion

The findings from these analyses suggest that $_{mol}$FOI was the most important variable associated with the rate of *Pf* malaria incidence in PNG children. $_{mol}$FOI was also useful as an outcome measurement for determining the incidence of *Pf* infections in a geographic area. Not surprisingly, clinical episodes and $_{mol}$FOI rates both peaked during the rainy season, so increasing interventions at the end of the dry season might be advisable.

The quadratic relationship between $_{mol}$FOI and age is consistent with previous findings, where the number of infective bites increased with body size (Port et al., 1980; Smith et al., 2006). Furthermore, PNG vectors are known to readily bite outdoors and in the early hours of the night (Charlwood et al., 1986; Hii et al., 1997), thus older children who are more independent may be at higher risk of being bitten when outdoors.

ITNs offer protection by limiting exposure to mosquitoes and by increasing mosquito mortality. Lengeler et al. (2004) estimated that ITN use reduced the incidence of uncomplicated malaria in areas of stable transmission by 50% compared to no nets. We estimated that ITN use resulted in a reduction in $_{mol}$FOI of 49%. ITN use in this group of children was effective in reducing $_{mol}$FOI, which was shown to be the most important predictor of clinical episodes.

Various studies from PNG (Charlwood et al., 1986; Hii et al., 1997; Burkot et al., 1988; Cattani et al., 1986) and other areas of endemic malaria (Woolhouse et al., 1997; Bejon et al., 2010) have shown that transmission can be highly variable even at a small spatial scale. Consequently, it was not surprising that $_{mol}$FOI varied both between villages and between children living within the same village.

Differences in $_{mol}$FOI likely affect prevalence and MOI as well as clinical disease, therefore it was not surprising that these measures showed the same age trend and association with ITN use (Figure 2.1). Although all three outcomes showed significant seasonal variation, we found that prevalence peaked earlier in the rainy season (end of January) than MOI (mid February) and $_{mol}$FOI (beginning of March).

An essential precondition for accurate estimation of both MOI and $_{mol}$FOI in large field studies is accurate molecular typing. The use of capillary electrophoresis for sizing the highly

polymorphic marker gene msp2 (Falk et al., 2006; Schoepflin et al., 2009) made it possible to precisely track parasite clones in consecutive blood samples; however, we recognize that some clones might have been missed in one or more blood samples. The possibility of adapting these techniques to a 96-well format and higher throughput makes it conceivable to routinely apply molecular parameters as outcome measures.

Some parasite clones inevitably remain undetected due to sequestration or densities fluctuating around the detection limit of PCR (Koepfli et al., 2011; Bretscher et al., 2010). This imperfect detectability of *Pf* infections can bias estimates of $_{mol}$FOI and should be considered if the intention is to comprehensively quantify parasite dynamics (Smith et al., 1999; Smith and Vounatsou, 2003; Sama et al., 2005). The detectability of a given msp2 genotype in a single blood sample from this study was estimated to be 79% (Koepfli et al., 2011). Therefore, we concluded that the sensitivity of detection by PCR did not seem to impair our estimate of the effect of $_{mol}$FOI on malaria incidence. Similarly, the use of additional marker genes would result in the detection of additional strains, and thus a higher MOI and $_{mol}$FOI. However, the use of several makers for estimating $_{mol}$FOI entails further statistical challenges because of the need to determine individual haplotypes, making it difficult to quantify MOI or to follow individual haplotypes over time.

Based on our findings, we propose the use of molecularly determined FOI as a major parameter in malaria surveillance, for monitoring of antimalarial interventions and for mathematical modeling of the impact of control measures on clinical epidemiology. In the context of malaria vaccine trials, $_{mol}$FOI potentially offers the chance to assess vaccine efficacy in the natural non-drug treated situation and may help to reduce sample size in clinical trials.

2.5 Analysis of *Pv* infections and clinical episodes

Pv infections were determined by genotyping the molecular markers msp1F3 and MS16 using capillary electrophoresis. Both markers proved to be highly polymorphic in the cohort with an expected heterozygosity (He) of 97.8% for MS16 and 88.1% for msp1F3. Details of the genotyping have been described previously (Koepfli et al., 2011). Clinical episodes attributed to *Pv* parasites were defined as light microscopically detected parasitemia greater than 500 parasites per μl and a body temperature greater than 37.5 degrees Celsius.

Pv parasites have the ability to remain dormant in the liver for long periods of time, sometimes up to several years. This is in contrast to *Pf* parasites that present in the blood within one to two weeks of an infective mosquito bite. For this reason, we will refer to the rate of acquisition of new *Pv* clones as the force of blood stage infection ($_{mol}$FOB) in this section, but we still intend to treat the variable as a measure of transmission intensity.

Pv infections that present in the blood after a long period in the liver are referred to as relapsing clones. Genotyping cannot directly identify relapses, so $_{mol}$FOB measures the combination of primary blood stage infections and those caused by relapsing clones. Therefore, homologous (same genotype) relapses occurring in two subsequent eight weeks intervals would be misclassified as persisting clones. New Guinean *Pv* strains are known to relapse rapidly (White, 2011); however in regions of high transmission, relapsing clones are usually of a different genotype than the initial blood stage infection (Imwong et al., 2007). Consequently, the number of homologous relapses that were not detected in a previous sample is expected to be relatively small. *Pv* $_{mol}$FOB was calculated by counting the number of msp1F3 and MS16 genotypes in each blood sample from an eight weeks interval that had not been present in the preceding interval blood sample.

2.5.1 *Pv* prevalence

All but five children had at least one *Pv* msp1F3 or MS16 PCR positive sample during the 16 months of followup. Of all samples collected, 51.6% and 52.7% were positive for msp1F3 and MS16, respectively, and 54.8% were positive for either marker. Of the 1,448 *Pv* positive samples, 2,305 and 3,372 distinct clones were detected by genotyping msp1F3 (65 different alleles) and MS16 (113 different alleles), respectively.

2.5.2 *Pv* $_{mol}$FOB

Over the entire followup, 9.6 new *Pv* msp1F3 clones and 14.0 new MS16 clones were found per child per year, calculated as the sum of the unique clones divided by the sum of the years-at-risk for all children. When both markers were combined, 15.3 *Pv* clones were observed per child per year.

Pv $_{mol}$FOB showed a very pronounced seasonality (Table 2.4, sin(week) IRR 0.99, cos(week) IRR 1.23), peaking in early January (week 1, 17.1 clones per year-at-risk), with the low season in early July (week 27, 11.3 clones per child per year; Figure 2.3 row 1, column 2). $_{mol}$FOB was also significantly lower in 2007 compared to 2006 (Table 2.4 IRR 0.84). Regular ITN use was associated with a significant reduction in acquisition of new clones (Table 2.4 IRR 0.66). A child with recent antimalarial treatment in the preceding four weeks had a higher $_{mol}$FOB than when that same child was not treated (Table 2.4 IRR 1.24). $_{mol}$FOB did not vary significantly with age. There was significant variation in $_{mol}$FOB between children in a village but not between villages (Table 2.4 random effects).

Table 2.4: Parameter estimates from GLMMs for *Pv* $_{mol}$FOB and clinical episodes.

				Malaria incidence					
	$_{mol}$FOB			model excluding $_{mol}$FOB			Model including $_{mol}$FOB		
	IRR	**95% CI**	**p value**	**IRR**	**95% CI**	**p value**	**IRR**	**95% CI**	**p value**
Fixed effects									
Age (at interval)				0.55	[0.46, 0.67]	< 0.001	0.52	[0.44, 0.62]	<0.001
Season									
Sin (week)	0.99	[0.93, 1.05]	<0.001	0.89	[0.77, 1.03]	<0.001	0.94	[0.81, 1.09]	<0.001
Cos (week)	1.23	[1.18, 1.29]	<0.001	1.45	[1.25, 1.67]	<0.001	1.24	[1.07, 1.44]	<0.001
ITN use	0.66	[0.56, 0.77]	<0.001						
Treated in past 28 days	1.24	[1.16, 1.33]	<0.001						
Year (2007)	0.84	[0.77, 0.92]	0.002						
($_{mol}$FOB)$^{1/3}$							1.99	[1.80, 2.19]	<0.001
Random effects	**Variance**			**Variance**			**Variance**		
Village	0.007		0.3	0.2		<0.001	0.35		<0.001
Child	0.2		<0.001	0.56		<0.001	0.28		<0.001
Seasonal effects									
Amplitude	0.21			0.39			0.22		
Month of peak	early January			early December			early December		
Month of trough	early July			early June			early June		

2.5.3 Clinical episodes of malaria caused by *Pv* parasites

Pv was the second most common cause of malarial illness, causing 605 episodes (IR 2.5 per child per year) with any parasite density. Of these, 391 episodes (IR 1.6 per child per year) fulfilled the more specific definition of *Pv* malaria (i.e. febrile illness plus *Pv* parasitemia >500 parasites/μl).

Age and season were significant predictors of clinical episodes of *Pv* malaria (Table 2.4 episodes >500). The incidence of *Pv* malaria decreased log-linearly with age (Figure 2.3, row 2, column 1; Table 2.4 IRR 0.55), from 2.9 episodes per child per year at one year of age to a minimum of 0.6 episodes per child per year at 3.5 years of age. It peaked at the beginning of the rainy season (early December, week 49, 1.7 clinical episodes per child per year; Figure 2.3, row 2, column 2) and was lowest in the early dry season (early June, week 23, 0.8 clinical episodes per child per year). ITN use was not significantly associated with incidence of *Pv* malaria. The incidence of *Pv* malaria varied significantly between villages and between children living in the same village (Table 2.4 >500 episodes, random effects).

When $_{mol}$FOB was added to the model, it was significantly positively associated with the incidence of *Pv* malaria (Table 2.4, 1.99). Adjusting for $_{mol}$FOB resulted in a 45% decrease in the effect of season on *Pv* incidence (Table 2.4, amplitude; Figure 2.4). Contrary to what was observed for *Pf*, adding *Pv* $_{mol}$FOB did not significantly alter the association of age or ITN use with incidence of clinical *Pv* episodes. Comparable results were seen when *Pv* episodes with any parasite density were considered (data not shown).

2.5.4 Discussion

The speed of acquisition of immunity to malaria parasites depends on transmission intensity (Koch, 1900; Snow et al., 1997) and is species-dependent, with immunity to *Pv* appearing to be acquired faster than immunity to *Pf* (Ciuca et al., 1934; Jeffery, 1966). In numerous field studies conducted in areas co-endemic for both species, the burden of *Pv* infections was found to peak at a younger age than those caused by *Pf* (Michon et al., 2007; Gunewardena et al., 1994; Maitland et al., 1996; Phimpraphi et al., 2008; Mueller et al., 2009).

The mechanisms underlying the immunity to malaria are not entirely understood (Doolan et al., 2009; Langhorne et al., 2008). Differences in the rate of natural acquisition of immunity to *Pf* and *Pv* may be the result of differences in the immune responses induced by either species, and/or by different numbers of infections acquired over time.

By genotyping all blood stage parasites detected over 16 months of followup, this study has provided the first direct estimate of the molecular force of *Pv* blood stage infections. Children acquired more than twice as many *Pv* clones per year than *Pf*. Differences between *Pv* and *Pf* were not only evident in the rate of acquisition of infections, but also in the associations between $_{mol}$FOB and incidence of clinical episodes and $_{mol}$FOB and age. *Pf* $_{mol}$FOI and incidence of malaria increased with age, whereas *Pv* $_{mol}$FOB did not change with age and was negatively associated with incidence of malaria.

Minor differences in the typing techniques applied for these two *Plasmodium* species could account for some differences in the estimates. Typing was based on length polymorphic marker genes. Their diversity was high, yet slightly differed: *Pf* was typed using msp2 (expected heterozygosity HE=0.933) (Schoepflin et al., 2009), while msp1F3 (HE=0.881) and MS16 (HE=0.978) were used for *Pv* typing (Koepfli et al., 2011). We determined the clone detectability for all three markers, defined as the proportion of clones detected in both of two bleeds collected 24 hours apart. Detectability differed between markers: 79% for Pfmsp2, 61% for PvMS16 and 73% for Pvmsp1F3 (Koepfli et al., 2011). The overall diversity of the Pfmsp2

Figure 2.3: Exploratory figures using smooth splines for relating age, seasonal patterns, and ITN use to *Pv* $_{mol}$FOB and clinical episodes.

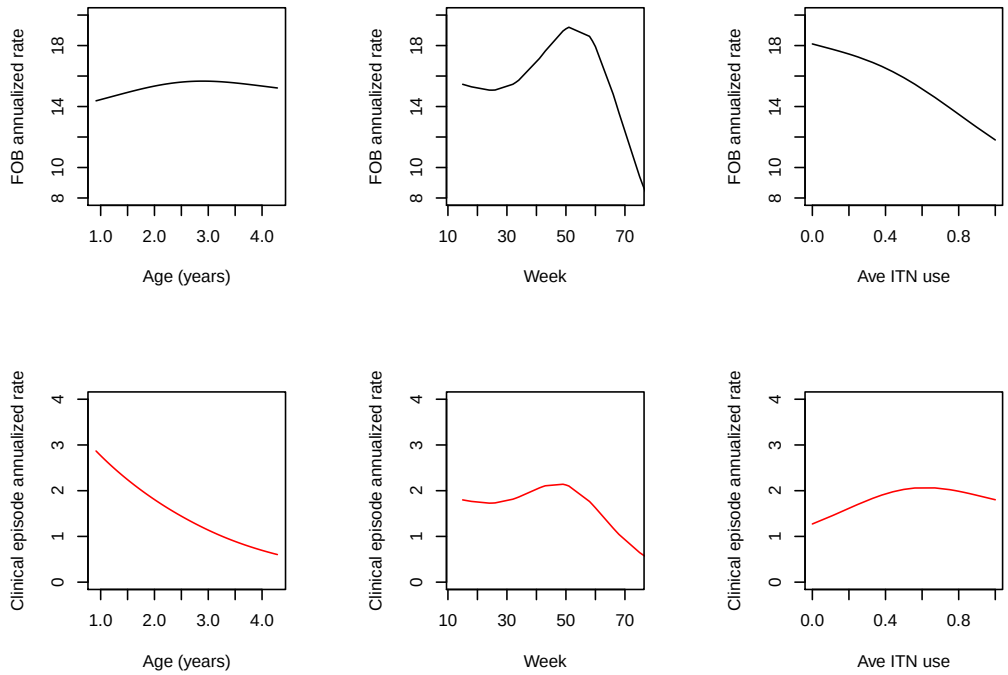

Figure 2.4: Incidence rate ratios for season (first week of the year reference) by incidence of *Pv* malaria, before (blue) and after (red) adjusting for $_{mol}$FOB.

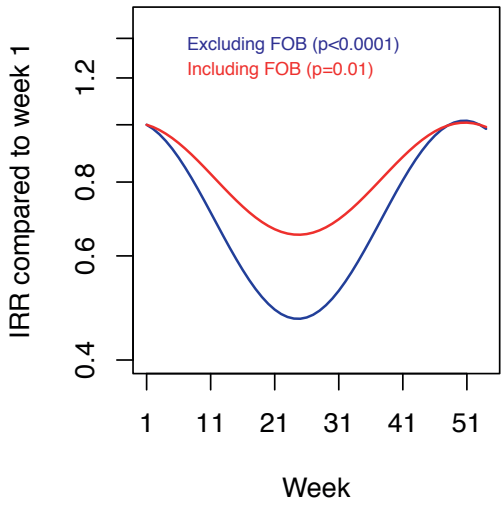

marker was similar to the two *Pv* markers, but Pfmsp2 detectability was higher. The most obvious difference in typing strategies was that our analysis of *Pv* was based on two loci, with the combined $_{mol}$FOB determined from maximal number of alleles per sample observed by any marker. Thus, the ability to detect clones of both *Pv* markers combined was higher than by the single *Pf* marker.

As a consequence of relapses, $_{mol}$FOB is not entirely equivalent to $_{mol}$FOI. *Pf* $_{mol}$FOI is directly linked to transmission intensity in a given interval, whereas *Pv* $_{mol}$FOB represents both transmission intensity and frequency and genetic complexity of relapsing parasites (some of which may have been acquired months or years earlier). Although *Pv* $_{mol}$FOB is not a direct measure of $_{mol}$FOI, the difference between the two measures is small if the total followup period is substantially longer than the average relapse frequency. In the Southwest Pacific, *Pv* infections are thought to relapse very rapidly - within a few weeks (White, 2011), so *Pv* $_{mol}$FOB is a good surrogate marker for $_{mol}$FOI if calculated over the entire 16 months of followup.

The effects of age on incidence of clinical disease caused by *Pv* and *Pf* estimated in this study parallel earlier findings in PNG (Michon et al., 2007; Mueller et al., 2009; Kasehagen et al., 2006) and other regions where both species are co-endemic (Gunewardena et al., 1994; Maitland et al., 1996; Phimpraphi et al., 2008). Our findings suggest that acquisition of immunity to *Pv* happens at a younger age than *Pf*. As immunity to malaria builds up gradually and is thought to be strain-specific (Ciuca et al., 1934; Jeffery, 1966), it is likely that the number of distinct infections acquired over an individual's lifetime is a major driving force for acquisition of immunity (Smith et al., 1999). The high exposure to *Pv* in this study may have been sufficient for children to acquire a certain degree of immunity against *Pv* infections as they aged. Furthermore, the lack of association between *Pv* $_{mol}$FOB and age suggests that, in older children, some of the *Pv* sporozoites transmitted by mosquitoes do not succeed in establishing detectable blood stage infections.

We propose that the high number of genetically distinct *Pv* blood-stage infections acquired in the first four years of life (as measured by $_{mol}$FOB) might contribute to the rapid acquisition of immunity to clinical *Pv* malaria. Although it is less closely linked to transmission, $_{mol}$FOB was a good measure of individual exposure to *Pv* blood-stage infection and was significantly linked to the observed burden of *Pv* malaria. As such, it could be used as both a surrogate maker for exposure and as a parameter for monitoring the impact of antimalarial interventions.

2.6 Acknowledgements

We would like to thank the study participants and their parents or legal guardians, and the field teams of the PNG Institute of Medical Research. The PNG study was supported by the Swiss National Science Foundation (grant no: 31003A-112196) and the National Institutes of Health (AI063135, AI-46919, and TW007872). The *Pf* results presented in this chapter were published in the *Proceedings of the National Academy of Sciences*, 2012 (Mueller et al., 2012). The *Pv* results will soon be published.

3 A bivariate Poisson lognormal model for estimating a measure of association between concurrent *Pf* and *Pv* infections

3.1 Mixed infections

In research focused on infectious diseases, it is common to observe infection with a particular pathogen accompanied by infection with a second type of pathogen or a different species of the same pathogen (e.g., multiple dengue serotypes, HIV and other sexually transmitted diseases, hepatitis B and C). Some typical approaches to estimating the risk of concurrent infections include simple chi-squares and correlation coefficients, linear models with one infection as the response and the other as the predictor and multinomial response models (Backus et al., 2005; Maurer and Sturchler, 2000; Coovadia and Wilkinson, 1998). McCulloch (2008) provides a nice summary of the advantages of joint modeling of responses, such as the ability to estimate the overall effects of important covariates on multiple outcomes, avoidance of multiple testing, efficiency gains and estimation of association between outcomes. This last point, estimating a measure of association between two responses, was one of the primary objectives of the PNG cohort study described in the previous chapters.

In PNG, children are perennially exposed to both *Pf* and *Pv* malaria parasites, and to this point, the relationship between the two species has not been measured in individuals that are coinfected. We investigate two measures of malaria burden from the PNG study to motivate the use of bivariate models for estimating association. The first measure of burden is the number of newly acquired genetically unique malaria infections over a period of observation. The second measure of burden is the number of *Pf* and *Pv* clinical episodes experienced over a period of time. We will relate these measures in separate bivariate models, comparing the counts for each of the two species. Thus, we present a bivariate model comparing *Pf* and *Pv* infections and a bivariate model for clinical episodes caused by *Pf* and *Pv* parasites. Recall that in Chapter 2 we made the distinction between $_{mol}$FOI and $_{mol}$FOB. In this chapter, we will refer to the rates of acquisition of new clones of *Pf* and *Pv* as $_{mol}$FOI, but keep in mind that these are measures of blood stage infections.

We begin by describing univariate Poisson and lognormal distributions that will be compounded to create the Poisson lognormal mixture distribution (Preston, 1948). We then show how this distribution can be adapted to a bivariate distribution with an association parameter using the approach first described by Aitchison and Ho (1989). A simulation study is then presented to compare two available methods for estimating the parameters of a bivariate Poisson lognormal model (BPLM). Finally, we fit BPLMs to the PNG data.

3.2 Statistical models

We will first describe the univariate Poisson lognormal (PL) mixture distribution. Ultimately, the BPLM will be implemented to estimate the association between the two responses caused by the two species of malaria. The BPLM was chosen because it permits negative association. There is some evidence that suggests the two species might be antagonistic; therefore, it was imperative that we fit a model that allowed the association parameter to be negative (Snounou and White, 2004; Mayxay et al., 2004; Smith et al., 2001).

3.2.1 Univariate Poisson lognormal distribution

In this section, we describe a univariate PL distribution, which is a mixture distribution derived from a Poisson distribution with a lognormal mean. Let Y represent a count of clinical episodes experienced by a child over a 16-week interval. The probability that a child will experience y episodes, given $\lambda > 0$, will be represented by a Poisson distribution,

$$P(Y = y|\lambda) = \frac{e^{-\lambda}\lambda^y}{y!} \qquad y = 0, 1, \ldots. \tag{3.1}$$

Furthermore, suppose that $\log(\lambda) \sim N(\mu, \sigma^2)$. This mixture forms the PL distribution,

$$\begin{aligned} P(Y = y|\mu, \sigma^2) &= \int_0^\infty P(Y = y|\lambda, \mu, \sigma^2)P(\lambda|\mu, \sigma^2)d\lambda \\ &= \int_0^\infty \frac{e^{-\lambda}\lambda^{y-1}}{y!}\frac{1}{\sigma\sqrt{2\pi}}e^{-(\log\lambda-\mu)^2/2\sigma^2}d\lambda. \end{aligned} \tag{3.2}$$

To simplify this distribution, it is convenient to write $\lambda = e^{\mu+\sigma Z}$, where $Z \sim N(0, 1)$. This results in a transformation of the lognormal mixture component into a standard normal distribution. Therefore, the PLM can be expressed as a mixture of Poisson distributions conditional on μ and σ,

$$P(Y = y|\mu, \sigma) = \int_{-\infty}^\infty \frac{\exp(y(\mu + \sigma z) - e^{\mu+\sigma z})}{y!}\frac{1}{\sqrt{2\pi}}e^{-z^2/2}dz, \tag{3.3}$$

and thus the Ys are observations from a Poisson distribution given Z. There is no simpler expression for the PL probability distribution. However, we can still calculate the moments using the moment generating function (mgf) of the normal, or in this case, after the transformation in (3.3), the mgf of the standard normal, $m(t) = \exp(\frac{1}{2}t^2)$,

$$\mathbb{E}(Y) = \mathbb{E}[\mathbb{E}(Y|Z)] = \mathbb{E}(\lambda) = e^\mu\,\mathbb{E}(e^{\sigma Z}) = e^{\mu+\sigma^2/2}. \tag{3.4}$$

It is clear from (3.4) that the PL reduces to the Poisson when $\sigma^2 = 0$.

The variance of the PL distribution is equal to the sum of the variance of the conditional mean and the mean of the conditional variance,

$$\begin{aligned} \mathrm{Var}(Y) &= \mathrm{Var}[\mathbb{E}(Y|Z)] + \mathbb{E}[\mathrm{Var}(Y|Z)] \\ &= \mathbb{E}(\lambda^2) + \mathbb{E}(\lambda) - [\mathbb{E}(\lambda)]^2 \\ &= e^{2\mu+2\sigma^2} + e^{\mu+\sigma^2/2} - e^{2\mu+\sigma^2} \\ &= e^{\mu+\sigma^2/2}\{1 + e^{\mu+\sigma^2/2}[e^{\sigma^2} - 1]\}. \end{aligned} \tag{3.5}$$

The PL distribution is useful because it does not require that the mean and variance be equal. In fact, the variance will always be larger than the mean with the PL distribution compared to the Poisson distribution, as we've just shown in (3.5). This is often referred to as overdispersion.

3.2.2 Bivariate Poisson lognormal distribution

When two outcomes are measured on the same unit over the same period of time, it is relatively straight forward to adapt their univariate distributions to a bivariate distribution. Let's again use counts of clinical episodes as an example, but now we have clinical episodes classified as having been caused by two different species of parasites. If these counts follow PL distributions, in other words, if the two λs for each of the counts follow lognormal distributions, then we can easily expand the univariate PLMs into a BPLM with correlation.

Let Y_1 and Y_2 represent the counts of clinical episodes caused by the two species with means λ_1 and λ_2 following lognormal distributions, respectively. Furthermore, write $\lambda_1 = e^{\mu_1+\sigma_1 U_1}$ and $\lambda_2 = e^{\mu_2+\sigma_2 U_2}$, where $U_1 = Z_1$ and $U_2 = \rho Z_1 + (1-\rho^2)^{1/2} Z_2$ and $Z_1 \perp Z_2 \sim N(0,1)$. The BPL distribution can be expressed as

$$\begin{aligned} &P(Y_1 = y_1, Y_2 = y_2 | \mu_1, \mu_2, \sigma_1, \sigma_2, \rho) \\ &= \int_{-\infty}^{\infty}\int_{-\infty}^{\infty} \frac{\exp(y_1(\mu_1+\sigma_1 u_1) - e^{\mu_1+\sigma_1 u_1})}{y_1!} \frac{\exp(y_2(\mu_2+\sigma_2 u_2) - e^{\mu_2+\sigma_2 u_2})}{y_2!} \\ &\quad \times \frac{1}{2\pi\sqrt{1-\rho^2}} \exp\Big\{ -\frac{1}{2(1-\rho^2)}\Big[u_1^2 + u_2^2 - 2\rho u_1 u_2\Big]\Big\} du_1 du_2. \end{aligned} \tag{3.6}$$

The marginal means are $\mathbb{E}(Y_1) = e^{\mu_1+\sigma_1^2/2}$ and $\mathbb{E}(Y_2) = e^{\mu_2+\sigma_2^2/2}$. The marginal variances are $\mathrm{Var}(Y_1) = e^{2\mu_1+\sigma_1^2}(e^{\sigma_1^2}-1) + e^{\mu_1+\sigma_1^2/2}$ and $\mathrm{Var}(Y_2) = e^{2\mu_2+\sigma_2^2}(e^{\sigma_2^2}-1) + e^{\mu_2+\sigma_2^2/2}$. Thus, under the assumed bivariate distribution, Y_1 and Y_2 are independent given U_1, U_2.

The covariance of Y_1 and Y_2 is

$$\begin{aligned} \mathrm{Cov}(Y_1, Y_2) &= \mathrm{Cov}[\mathbb{E}(Y_1|U_1), \mathbb{E}(Y_2|U_2)] + \mathbb{E}[\mathrm{Cov}(Y_1, Y_2|U_1, U_2)] \\ &= \mathrm{Cov}[e^{\mu_1+\sigma_1 U_1}, e^{\mu_2+\sigma_2 U_2}]. \end{aligned} \tag{3.7}$$

Using the mgf of the bivariate normal we get

$$\mathbb{E}(e^{\mu_1+\sigma_1 U_1} e^{\mu_2+\sigma_2 U_2}) = \exp(\mu_1+\mu_2)\exp\Big(\frac{1}{2}(\sigma_1^2 + 2\rho\sigma_1\sigma_2 + \sigma_2^2)\Big), \tag{3.8}$$

and thus,

$$\begin{aligned} \mathrm{Cov}(Y_1, Y_2) &= \exp(\mu_1+\mu_2)\exp\Big(\frac{1}{2}(\sigma_1^2 + 2\rho\sigma_1\sigma_2 + \sigma_2^2)\Big) - \exp(\mu_1+\sigma_1^2/2)\exp(\mu_2+\sigma_2^2/2) \\ &= \Big\{\exp\Big(\mu_1+\mu_2+\frac{1}{2}(\sigma_1^2+\sigma_2^2)\Big)\Big\}(\exp(\rho\sigma_1\sigma_2) - 1). \end{aligned} \tag{3.9}$$

Finally, the correlation is

$$\begin{aligned}\rho_{Y_1Y_2} &= \frac{\text{Cov}(Y_1, Y_2)}{\sqrt{\text{Var}(Y_1)}\sqrt{\text{Var}(Y_2)}} \\ &= \frac{\{\exp(\mu_1 + \mu_2 + \frac{1}{2}(\sigma_1^2 + \sigma_2^2))\}^{1/2}(\exp(\rho\sigma_1\sigma_2) - 1)}{\sqrt{1 + \exp(\mu_1 + \sigma_1^2/2)[\exp(\sigma_1^2) - 1]}\sqrt{1 + \exp(\mu_2 + \sigma_2^2/2)[\exp(\sigma_2^2) - 1]}}\end{aligned} \tag{3.10}$$

(Aitchison and Ho, 1989).

3.3 A simulation study

In this section, we present a simulation study to evaluate two methods of estimating the parameters of a BPLM. We first generate data from a BPL distribution using parameter estimates that mimic the PNG data. Next, we introduce an integral approximation method called Adaptive Gaussian Quadrature and a Bayesian method that uses Markov chain Monte Carlo (MCMC) methods to estimate the posterior distributions of the parameters of the BPLM. We compare these two algorithms by fitting them to the simulated data.

3.3.1 Generating data from a BPL distribution

We generated 1,000 sets of 200 (Y_1, Y_2) pairs of Poisson random variables with means $\lambda_1 = \exp(\mu_1 + \sigma_1 U_1 + \log(t))$ and $\lambda_2 = \exp(\mu_2 + \sigma_2 U_2 + \log(t))$, where $U_1 = Z_1$ and $U_2 = \rho Z_1 + (1 - \rho^2)^{1/2} Z_2$ and $Z_1 \perp Z_2 \sim N(0, 1)$, for a set of parameter values (Table 3.1). The first simulation described in Table 3.1 was conducted so that the parameter values produced Ys that were similar to the counts of clinical episodes caused by the two species in the PNG data. These were very small counts that ranged between zero and five clinical episodes per child per 16 weeks interval, with most of the observations equal to zero or one. The second simulation described in Table 3.1 was conducted so that the Ys were distributed similarly to the number of newly acquired infections, or $_{mol}$FOIs, for the two species in the PNG data. These counts ranged between zero and 15. We generated a time-at-risk variable, denoted t, which was distributed similar to the years-at-risk in the PNG data, specifically $t \sim N(0.25, 0.06)$. The variable t was then used as an offset in the BPLMs, which was done by adding $\log(t)$ to the means, as shown in the first sentence of this paragraph.

3.3.2 Fitting a BPLM to simulated data

We fit BPLMs to the simulated data using two different algorithms. The first algorithm was fit using the NLMIXED procedure in SAS (SAS Institute, 2013). The NLMIXED procedure maximizes an approximation to the likelihood integrated over the overdispersion parameters. We chose Adaptive Gaussian Quadrature (Pinheiro and Bates, 1995) for the integral approximation and the dual Broyden, Fletcher, Goldfarb, and Shanno (DBFGS) update of the Cholesky factor of the Hessian matrix optimization method, which is a quasi-Newton method. By default, with this model specification, NLMIXED computed the approximate standard errors by the delta method. The starting values for the parameters were set at the values used to generate the data. The second method was fit using the MCMCglmm package (Hadfield, 2010) in R. The MCMCglmm package fits various types of linear and GLMMs using MCMC techniques. It also fits overdispersed univariate and bivariate Poisson models. The algorithm uses a combination of Gibbs sampling, slice sampling and Metropolis-Hastings to move the chain through

the parameter space. We specified a multivariate inverse Wishart prior for the overdispersion parameters, $\sigma_1, \sigma_2 \sim IW([0.002, 0.002], \mathbf{\Sigma})$, where the diagonal values of $\mathbf{\Sigma}$ were equal to one and the off-diagonal values were equal to zero. This prior assumed *a priori* independence between the σs; however, a fully parameterized covariance matrix was estimated from the model fit by the following

$$\mathbf{\Sigma} = \begin{bmatrix} \sigma_1^2 & \rho\sigma_1\sigma_2 \\ \rho\sigma_1\sigma_2 & \sigma_2^2 \end{bmatrix}.$$

A multivariate normal prior with zero means and large variances (1E6) was specified for the μs. For each simulation, the univariate fits used 10,000 iterations with a burn-in period of 1,000 and a thinning interval of 20, and the bivariate fits used 20,000 iterations with a burn-in period of 2,000 and a thinning interval of 20.

The simulation results from both methods for both sets of response variables are summarized in Table 3.1. The columns are defined by the following

$$\text{Bias}(\hat{\theta}) = \frac{1}{n}\sum_{i=1}^{n}\hat{\theta}_i - \theta \tag{3.11}$$

$$\text{RMSE}(\hat{\theta}) = \sqrt{\frac{1}{n}\sum_{i=1}^{n}(\hat{\theta}_i - \theta)^2} \tag{3.12}$$

$$\text{RMS}(\hat{\text{SE}}) = \sqrt{\frac{1}{n}\sum_{i=1}^{n}(\hat{\text{SE}}_i^{\,2})}, \tag{3.13}$$

where θ is the value of the parameter used to simulate the data, $\hat{\theta}$ is the parameter estimate from each of the n=1,000 simulations and $\hat{\text{SE}}$ is the estimated standard error for each parameter from the 1,000 simulations. The standard errors from the MCMCglmm algorithm were calculated by subtracting the lower limit of the credible interval from the upper limit of the credible interval and dividing that value by four. This yielded similar but slightly higher estimates compared to taking the standard deviations of the posterior distributions.

Both algorithms did a poor job of estimating the parameters when the data were simulated so that the *Y*s followed the distributions of clinical episodes observed in the PNG data (simulation 1, Table 3.1). The estimates of ρ from both algorithms were especially disappointing, with both being approximately 50 percent underestimated. The standard errors were somewhat better estimated with the MCMC algorithm and were terribly off the mark when estimated using AGQ. The NLMIXED procedure failed to converge three out of the 1,000 simulations and experienced optimization errors that resulted in missing values for the standard errors more than 200 times for each parameter. The simulated counts were very small, and the *Y*s, reflective of clinical episodes caused by *Pf*, exhibited very little overdispersion (σ_1=0.4). The standard errors calculated by the NLMIXED procedure were extremely large for some fits (Table 3.1, RMS($\hat{\text{SE}}$)), which was further evidence that the algorithm struggled to correctly estimate the parameters. It is possible that the parameter estimates used to simulate the data were not representative of the true parameters of the PNG data generating distribution. Because they were chosen by fitting a BPLM to the PNG data, they could have been strongly influenced by single observations that produced high leverage. We will investigate this further when we present the results of fitting BPLMs to the PNG data later in this chapter.

The second simulation yielded much better results. Both algorithms produced results that suggested consistency with 1,000 simulations (simulation 2, Table 3.1). The distributions of counts of $_{mol}$FOIs were much greater than the counts of clinical episodes (Table 3.2), which

Table 3.1: Results from fitting BPLMs to 1,000 replicates of samples of size 200 simulated Y_1s and Y_2s using AGQ and MCMC methods. (All values multiplied by 100.)

	True θ	**Mean($\hat{\theta}$)**		**Bias($\hat{\theta}$)**		**RMSE($\hat{\theta}$)**		**RMS($\widehat{\text{SE}}$)**	
Parameter		**AGQ**	**MCMC**	**AGQ**	**MCMC**	**AGQ**	**MCMC**	**AGQ**	**MCMC**
Simulation 1[*]									
μ_1	40	36	34	-4	-6	14	16	15[‡]	11
σ_1	40	29	32	-11	-8	23	16	16375[‡]	12
μ_2	20	41	31	21	11	26	21	19[‡]	16
σ_2	90	87	93	-3	3	16	18	23[‡]	16
ρ	80	39	41	-41	-39	82	69	123[‡]	34
Simulation 2[†]									
μ_1	125	125	126	0	1	12	10	11	10
σ_1	76	74	81	-2	5	12	11	10	9
μ_2	265	265	261	0	-4	9	6	7	7
σ_2	72	71	72	-1	0	8	4	6	6
ρ	74	75	85	1	11	11	14	11	8

[*]Values produced Ys similar to clinical episode counts and [†]values produced Ys similar to the $_{mol}$FOI counts. [‡]Missing estimates of standard errors due to optimization errors.

might explain the improvements seen in the second simulation.

We fit univariate models to the simulated data to check that the parameter estimates did not change noticeably between the univariate and bivariate fits. Only one additional parameter was estimated in the bivariate models, so we would expect them to produce similar results. As expected, there were very small differences in the parameter estimates between the univariate and bivariate models for simulation 1 (Figure 3.1) and simulation 2 (Figure 3.2).

Figure 3.1: Changes in average parameter estimates between the univariate and bivariate models from simulation 1 across 1,000 simulations.

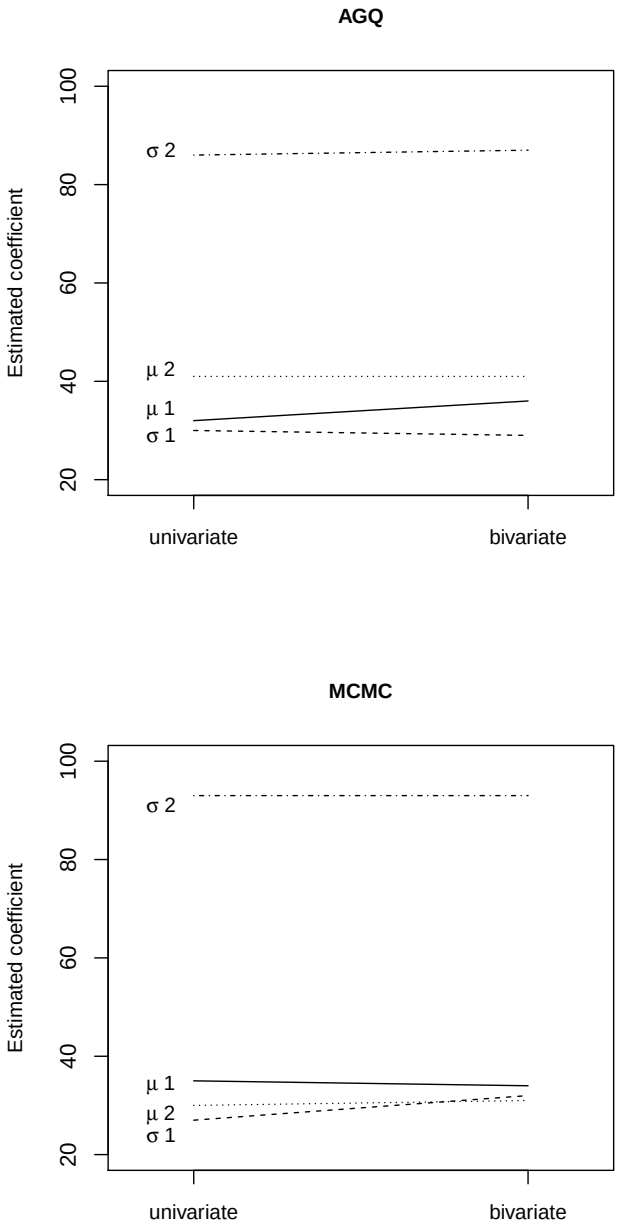

Figure 3.2: Changes in average parameter estimates between the univariate and bivariate models from simulation 2 across 1,000 simulations.

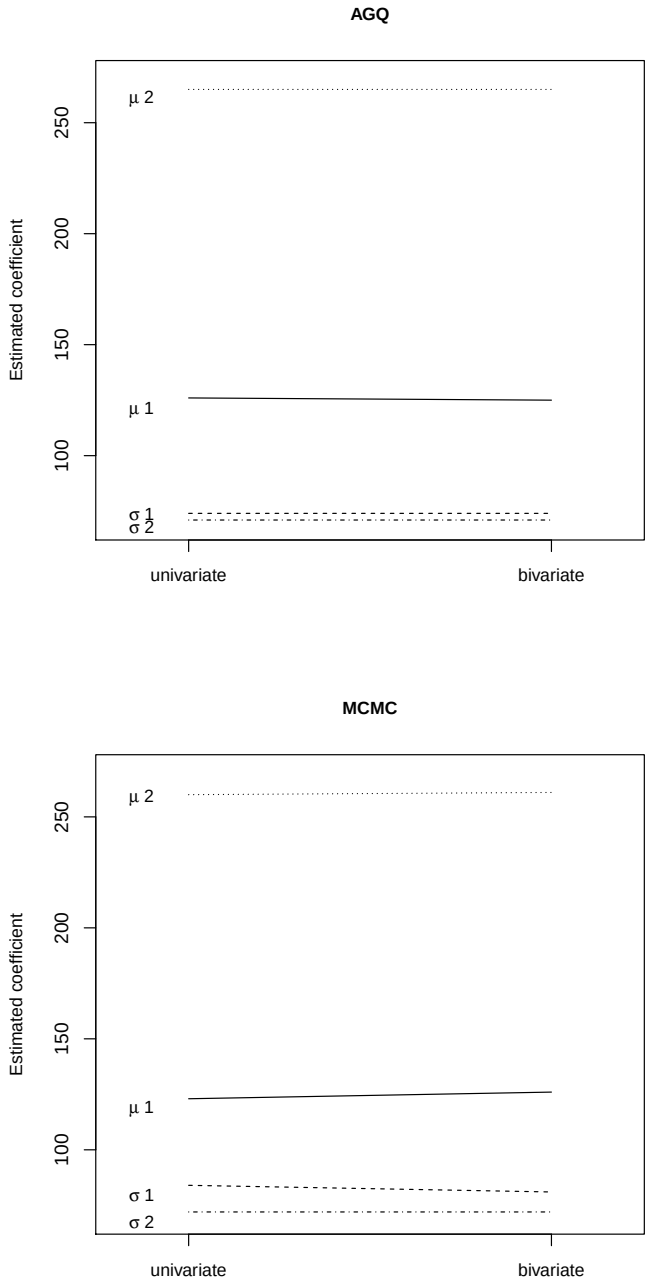

The simulation results for Ys reflective of $_{mol}$FOI counts were encouraging, as they showed small bias and consistent estimation of the standard errors. However, the results from fitting a BPLM to data imitating clinical episode counts showed large bias, inconsistencies across the estimation algorithms and inconsistent estimates of the standard errors. The NLMIXED procedure failed to converge and did not produce an estimate of ρ for almost 50 percent of the iterations. In the next section, we fit BPLMs to the PNG data by 16 weeks intervals. Diagnostic measures are presented to investigate influential observations.

3.4 Fitting BPLMs to the PNG data

We again used the PNG cohort data described in previous chapters. The children in this cohort were exposed to both *Pf* and *Pv* parasites and experienced clinical episodes attributable to each of these species at high rates throughout the study period (Table 3.2). Each febrile illness that was accompanied by blood samples containing *Pf* parasites (>2500 parasites/μl) and/or *Pv* parasites (>500 parasites/μl) determined by light microscopy was classified as having been caused by one or both species of parasite.

We combined the data into four 16 weeks intervals for each child. The data described in Chapter 2 were analyzed by eight eight-weeks intervals. We originally fit the BPLMs to the eight weeks interval data, but the clinical episode counts were very small and exhibited almost no overdispersion. Thus, the data in this chapter were aggregated over 16 weeks so that we could model larger counts.

We were interested in the rates at which children were getting sick with malaria, rather than simply the counts of clinical episodes. The distributions of clinical episode annualized rates were similar for both species (Table 3.2). However, there was one extreme observation in interval two for a child experiencing clinical episodes caused by *Pv*. This child experienced two *Pv* clinical episodes during the 16 weeks interval but was only at risk for 0.04 years. The average years-at-risk during an interval was 0.25.

Incidence rates of clinical episodes and $_{mol}$FOI are summarized by person-years-at-risk in Table 3.2 (e.g., total episodes/total years-at-risk for each interval). Confidence intervals for the rates were calculated using Haenszel et al.'s table (1962). Children most often experienced between one and three clinical episodes per year-at-risk for both species. However, children experienced much higher rates of new *Pv* infections compared to new *Pf* infections.

We wanted to determine the association between clinical episode counts and annualized rates caused by *Pf* and *Pv* and between *Pf* and *Pv* $_{mol}$FOI counts and annualized rates. To get a basic measure of the correlation, we calculated Kendall's τ rank correlation coefficients. These are summarized in Table 3.3.

There was no association between clinical episodes caused by *Pf* and those caused by *Pv* according to Table 3.3. However, there was a strong positive association between *Pf* and *Pv* $_{mol}$FOI. The estimates in Table 3.3 do not permit adjustments for covariates that are also related to the outcomes. The advantage of fitting a BPLM, is that it allows for estimation of the association between the two outcomes and estimation of the effects of the covariates on both outcomes simultaneously.

3.4.1 Malaria clinical episodes caused by *Pf* and *Pv* parasites

In previous analyses of these data, we determined that age, ITN use and $_{mol}$FOI were important predictors of clinical episode annualized rates caused by a particular malaria species (see Chapter 2). *Pv* parasites can remain dormant in the liver for long periods of time, sometimes up

Table 3.2: Average counts (IQR) and incidence rates per person-years-at-risk (95% CI) for clinical episodes and $_{mol}$FOI.

Variable	**Interval 1**	**Interval 2**	**Interval 3**	**Interval 4**
Pf clinical episodes				
count	0.4 (0, 1)	0.4 (0, 1)	0.7 (0, 1)	0.4 (0, 1)
rate	1.5 (1.2, 1.9)	1.7 (1.4, 2.1)	3.1 (2.7, 3.6)	1.3 (1.1, 1.7)
Pv clinical episodes				
count	0.4 (0, 1)	0.5 (0, 1)	0.5 (0, 1)	0.2 (0, 0)
rate	1.8 (1.4, 2.2)	2.0 (1.6, 2.4)	1.9 (1.6, 2.3)	0.8 (0.6, 1.1)
Pf $_{mol}$FOI				
count	1.3 (0, 2)	1.1 (0, 2)	2.0 (0, 3)	1.1 (0, 2)
rate	5.5 (5.0, 6.0)	4.4 (4.0, 4.8)	8.2 (7.5, 9.0)	3.9 (3.6, 4.3)
Pv $_{mol}$FOI				
count	3.6 (1, 5)	4.1 (2, 6)	4.4 (2, 7)	3.1 (1, 5)
rate	15.3 (14.2, 16.4)	17.0 (16.0, 18.1)	18.3 (17.2, 19.5)	11.2 (10.4, 12.0)

Table 3.3: Kendall's τ correlation coefficients (p-values) for clinical episode counts and annualized rates and $_{mol}$FOI counts and annualized rates caused by *Pf* and *Pv*.

	***Pf* and *Pv* clinical episodes**		***Pf* and *Pv* $_{mol}$FOI**	
Interval	**Counts**	**Rates**	**Counts**	**Rates**
1	0.05 (0.4)	0.06 (0.3)	0.19 (<.001)	0.16 (0.001)
2	-0.06 (0.3)	-0.003 (1.0)	0.24 (<.001)	0.20 (<.001)
3	-0.1 (0.1)	-0.02 (0.6)	0.15 (0.002)	0.14 (0.001)
4	0.06 (0.3)	0.1 (0.09)	0.09 (0.09)	0.11 (0.02)

to three years, unlike *Pf* parasites that usually appear in the blood within one to three weeks of a bite by an infective mosquito. *Pv* can thus establish new blood-stage infections in the absence of additional mosquito bites through the activation of such long-lasting liver stages, called the hypnozoites. For this reason, Pf_{mol}FOI is a better measure of recent exposure to infective mosquito bites than Pv_{mol}FOI. Both parasites are transmitted by the same mosquitoes, so it is permissible to use Pf_{mol}FOI as a surrogate measure of exposure to mosquito bites, and thus risk of experiencing clinical episodes caused by either species.

We fit BPLMs for clinical episode annualized rates with age, ITN use, and Pf_{mol}FOI as predictors for each interval using both AGQ and MCMC methods (Table 3.4). Extensive discussion of the relationships between the covariates and the marginal responses is covered in previous analyses. The objective of this analysis was to obtain an estimate of the association between the two responses while adjusting for variation attributable to covariates related to clinical episodes. Table 3.4 only includes estimates of the overdispersion parameters (σ:*Pf* and σ: *Pv*) and the association parameter, ρ. The coefficients for age, ITN use and Pf_{mol} are not shown, but these variables were included in the model fits. The estimates of the coefficients for these variables were very similar to those obtained from the analyses described in Chapter 2.

Table 3.4: Results from fitting BPLMs to clinical episode annualized rates by 16 weeks intervals using AGQ and MCMC. Models included age, ITN use and $_{mol}$FOI, but the coefficients for these variables are not shown. (All values multiplied by 100).

Method	**Interval 1**	**Interval 2**	**Interval 3**	**Interval 4**
AGQ				
σ: *Pf*	32.6 (3.1, 103.1)	1.8 (-, -)	1.8 (-, -)	30.2 (10.5, 111.1)
σ: *Pv*	68.1 (36.7, 144.4)	70.8 (44.8, 156.4)	60.5 (33.7, 140.1)	119.2 (82.5, 228.2)
ρ	59.4 (-100.0, 100.0)	0.4 (-, -)	40.4 (-, -)	100.0 (-, -)
MCMC				
σ: *Pf*	35.0 (8.5, 61.8)	16.5 (2.5, 36.6)	15.1 (3.0, 27.5)	30.8 (13.2, 49.0)
σ: *Pv*	64.8 (25.3, 105.0)	43.1 (4.1, 92.7)	57.9 (28.1, 90.5)	119.6 (79.9, 168.9)
ρ	40.1 (-98.8, 99.9)	-5.0 (-95.9, 99.8)	11.2 (-98.8, 99.5)	86.0 (18.9, 99.9)

Missing values (-) due to optimization errors.

The estimates of the fixed effect coefficients (not shown) and σs (Table 3.4) by AGQ and MCMC agreed acceptably well. There were considerable differences in the estimates of ρ between the two algorithms, especially in the credible (or confidence) intervals. The credible intervals were so wide that it was not worthwhile to interpret the results. The NLMIXED procedure failed to produce estimates of the standard errors for some of the σs and ρs in Table 3.4 due to optimization errors. It may be the case that this particular model did not fit the data well or there was simply no association between the two clinical episode rates. Furthermore, there might have been single observations that strongly influenced the parameter estimates.

Several model diagnostics were used to investigate the residuals and influence of specific observations on the parameter estimates using the MCMCglmm package. Plots of residuals for each of the marginal predicted values for clinical episodes caused by *Pf* and *Pv* are provided in the Appendix (Figure A1). For all of the parameters, there were large residuals, and most of them were in the negative direction, indicating that the fitted values were lower than the observed values. The range of fitted values across all intervals and species was zero to 1.2 clinical episodes, whereas the range of observed values was zero to five clinical episodes. This indicated that the parameter estimates produced negatively biased fitted values. The interquartile ranges of clinical episodes caused by both species were zero to one in the observed

data, thus the fitted values from the model were in an acceptable range of the majority of the distribution of observed episode counts, but the model did a poor job of estimating the tails of the distributions.

We also evaluated the parameter estimates from MCMCglmm by sampling a subset of the data and refitting the BPLMs 1,000 times. To do this, we sampled 90 percent of the observations without replacement and fit BPLMs to assess the change in the parameter estimates when a random sample of 10 percent of the observations were excluded. Figure A2 in the Appendix displays the distributions of the parameter estimates from the 1,000 samples by interval. There was substantial variability in the parameter estimates when random samples of 10 percent of the data were excluded over the 1,000 samples. The range of values on the x-axes of Figure A2 in the Appendix are all 140 units (the estimated parameter values were multiplied by 100). We expected that most of the histograms would look similar to that shown for the *Pf* intercept in interval three, with values clustering around the mean and with very little spread. However, many of the distributions show wide spread, which meant that the parameter estimates noticeably changed when 10 percent of the observations were excluded.

Considering the great number of observations with large residuals and the magnitude of changes in the parameter estimates when random samples of observations were excluded from the BPLM fits, the task of excluding outliers might prove to be arduous. The results of these model diagnostics leave us with doubt about whether precise estimates can be produced from these data and whether is it even possible to detect an association between the two highly variable measures of interest.

The MCMCglmm package and the NLMIXED procedure did a poor job of estimating ρ from the BPLMs, but the lack of overdispersion in the counts of clinical episodes caused by *Pf*, and the small counts of clinical episodes caused by the two species in general, were likely the culprits for this poor fit. Furthermore, there were many outliers in the distributions of annualized rates caused by both species, which led to very large confidence intervals for the estimates of σ_1, σ_2 and ρ.

3.4.2 Rate of acquisition of infections of malaria parasites

The secondary objective in this analysis was to estimate the relationship between the rate of acquisition of *Pf* and *Pv* parasites, or $_{mol}$FOI annualized rates. As described previously, Pv $_{mol}$FOI is not a direct measure of recent exposure to infective mosquito bites, rather, it is a measure of blood-stage infection caused by both primary and relapsing infections. Therefore, by fitting a BPLM to *Pf* and *Pv* $_{mol}$FOI, we were estimating the association between rates of new blood-stage infections of each parasite acquired during an interval.

To estimate the association between *Pf* and *Pv* $_{mol}$FOI, we fit BPLMs with age and ITN use as covariates using NLMIXED and MCMCglmm. The results are summarized by interval in Table 3.5. Again, only the estimates for the overdispersion parameters and ρ are provided.

There was a moderate positive association between *Pf* and *Pv* $_{mol}$FOI in the first three 16 weeks intervals. The estimates of ρ in Table 3.5 were a good indication of the association between *Pf* and *Pv* $_{mol}$FOI, but to calculate estimates of the correlation between the two responses, we used equation (3.10). The results from applying this formula to the parameter estimates in Table 3.5 are summarized in Table 3.6. The age and ITN coefficients were multiplied by the mean age and mean ITN use over all children during each specific interval, and these values were added to the intercepts in order to obtain the μs.

The estimates of correlation presented Table 3.6 were much higher than those obtained using Kendall's τ statistics (Table 3.3) and were significantly greater than zero for the first three

Table 3.5: Results from fitting BPLMs to $_{mol}$FOI annualized rates by 16 weeks intervals using AGQ and MCMC. Models included age and ITN use, but the coefficients for these variables are not shown. (All values multiplied by 100).

Method	**Interval 1**	**Interval 2**	**Interval 3**	**Interval 4**
AGQ				
σ: *Pf*	83.7 (64.3, 103.1)	54.0 (32.9, 75.1)	47.5 (33.6, 61.5)	69.5 (50.6, 88.4)
σ: *Pv*	69.9 (56.8, 82.9)	65.5 (54.7, 76.2)	58.0 (48.2, 67.9)	58.9 (47.0, 70.7)
ρ	35.0 (8.4, 61.7)	61.5 (28.1, 94.9)	43.4 (13.1, 73.6)	1.9 (-31.1, 35.0)
MCMC				
σ: *Pf*	85.6 (67.3, 106.3)	49.6 (32.3, 67.3)	47.3 (33.1, 61.2)	68.9 (48.9, 86.6)
σ: *Pv*	71.1 (57.4, 83.8)	67.1 (57.6, 79.1)	59.3 (49.1, 67.9)	59.8 (47.5, 71.5)
ρ	36.3 (9.3, 60.3)	71.8 (41.8, 93.9)	46.7 (15.9, 76.2)	3.4 (-30.5, 38.3)

Table 3.6: Estimates of the association between *Pf* and *Pv* $_{mol}$FOI using the parameter estimates from the BPLMs (Table 3.5) and equation (3.10). (All values multiplied by 100).

Method	**Interval 1**	**Interval 2**	**Interval 3**	**Interval 4**
AGQ	25.0 (3.8, 49.6)	39.1 (6.9, 87.0)	30.4 (4.9, 64.8)	1.1 (-7.4, 26.6)
MCMC	26.0 (4.4, 47.7)	44.2 (10.5, 83.8)	32.8 (6.1, 67.3)	2.0 (-7.1, 29.4)

intervals. The magnitude of the coefficients suggest that *Pf* and *Pv* $_{mol}$FOI were moderately positively correlated. The parameter estimates from the two algorithms were very similar, and the confidence intervals were much narrower than those estimated for clinical episodes. These parasites are transmitted by the same mosquitoes, and it is even possible for both to be transmitted simultaneously by a single mosquito bite (Snounou and White, 2004; McKenzie et al., 2006). There were higher rates of *Pv* infections (15.3 per child per year) in these children compared to *Pf* (5.4 per child per year), but there were more clinical episodes caused by *Pf* (1.9 per child per year) than those caused by *Pv* (1.6 per child per year) over the entire cohort. These findings indicate that children exposed to one species of parasite were at risk of acquiring clones of the other parasite during the same period of observation. Furthermore, in Chapter 2, it was determined that increased numbers of clones acquired over an interval resulted in increased rates of clinical episodes, which might be an indication that mixed infections were associated with clinical episodes. However, this analysis did not directly answer that question. We will address this question in more detail in Chapter 4.

It was not clear why the association was so much lower in interval 4 compared to the other intervals. The rates of new clones of both species were similar to the other intervals. This interval included the oldest children, and we established that there is reason to believe that immunity to *Pv* occurs at a younger age than immunity to *Pf*, but the age effects were similar to those estimated in the other three intervals. However, ITN use was much more effective in this interval, and the effect of ITN on *Pf* clones was more than twice that estimated for *Pv* clones. It is possible that because ITN use had such a dramatically different effect on *Pf* clones, the two rates were more dissimilar in this interval than other intervals.

3.5 Discussion

A BPLM was appropriate for relating *Pf* and Pv_{mol}FOI because both of these variables exhibited overdispersion and there was prior belief that they might be negatively associated. A BPLM was not appropriate for modeling clinical episodes in these data because the counts were very small and exhibited almost no overdispersion. A better model for relating clinical episodes caused by the two species might be a bivariate binomial model, where the clinical episode variables are coded as zero or greater than one episode during an interval.

The analysis of *Pf* and Pv_{mol}FOI suggested that the two species of malaria parasites were positively associated with one another. These results suggest that prevention programs in areas where both species are endemic should be targeted at eliminating both species. Although the burden of *Pv* malaria is typically considered to be less than that of *Pf* malaria, there were still a large number of clinical episodes attributable to *Pv* infections in this population, so it was certainly a burden to children in PNG and should not be ignored.

A BPLM fit by either the NLMIXED procedure in SAS or the MCMCglmm package in R is a valid method for estimating the correlation between two overdispersed Poisson variables. However, when the overdispersion parameters are very small and there is large variability in the dependent variables, it is advisable to test the algorithms on simulated data and carry out model diagnostics before attempting to draw firm conclusions.

4 Analyses pertaining to mixed infections

In this chapter, we estimate the effect of having *Pf* and/or *Pv* infections on rates of subsequent homologous (same species) or heterologous (of the opposite species) clinical episodes. Furthermore, we examine the relationship between the two species of infections and test whether this relationship is different in children with symptomatic or asymptomatic infections (as denoted by the presence or absence of febrile symptoms). We estimate these relationships using generalized linear mixed models (GLMMs).

4.1 Results

We again used the eight weeks interval data from the PNG cohort. Two blood samples were taken 24 hours apart at each eight weeks interval visit. Positive infections were defined as presence of a particular parasite in either of the blood samples. However, during the first and last visits, only one blood sample was taken for each child. Therefore, the analyses in this chapter where infection status was the response exclude the first and last intervals of data. Table 4.1 presents cross-tabulations of infections from visits two through seven stratified by presence of fever.

Table 4.1: Biological measurements from eight weeks interval blood samples stratified by presence of fever (excluding the first and last intervals where only one blood sample was obtained). Positive samples determined by PCR.

	Total	**Fever**
Variable	**N (%*)**	**N (%†)**
Fevers at eight weeks interval visits	310 (22)	
Single-species *Pf* infections	211 (15)	78 (37)
Single-species *Pv* infections	522 (36)	88 (17)
Mixed *Pf* and *Pv* infections	373 (26)	99 (27)

*Percent of eights weeks blood samples from intervals two through seven;†percent of infections with a fever.

Children experienced more single-species *Pv* infections than single-species *Pf* or mixed infections. Thirty-seven percent of children presenting with a single-species *Pf* infection also had a fever, whereas only 17% of children with a single-species *Pv* infection had a concurrent fever at the eight weeks visits. The results in Table 4.1 suggest that having a single-species *Pf* infection was associated with the greatest probability of concurrent fever. We will investigate this further in the next section.

4.1.1 Estimating the association between heterologous infections

Children in this cohort were repeatedly re-infected with multiple species of malaria parasites. We wanted to determine the relationship between *Pf* and *Pv* infections determined by PCR at the start of the interval. We again fit GLMMs with village and child random effects excluding the first and last intervals. Infection status for each species was binary, so we fit binomial GLMMs with the opposite species as a binary predictor. We also included a binary factor for current fever at the time of the blood sample to determine whether this affected the relationship between the two species of infections. Results are summarized in Table 4.2 (*Pf* infections by PCR) and Table 4.3 (*Pv* infections by PCR).

Table 4.2: Odds ratio estimates (95% CI) from GLMMs for predicting binary *Pf* infections determined by PCR.

	Model 1 **OR (95% CI)**	**Model 2** **OR (95% CI)**	**Model 3** **OR (95% CI)**
Fixed effects			
Intercept	0.10 (0.02, 0.48)	0.08 (0.02, 0.36)	0.07 (0.02, 0.35)
Age	5.08 (1.50, 17.21)	5.50 (1.60, 18.90)	5.36 (1.56, 18.4)
Age^2	0.78 (0.61, 0.99)	0.77 (0.61, 0.98)	0.77 (0.61, 0.99)
Sin(week)	1.55 (1.30, 1.84)	1.54 (1.29, 1.83)	1.54 (1.29, 1.83)
Cos(week)	1.39 (1.16, 1.65)	1.35 (1.13, 1.61)	1.35 (1.13, 1.61)
ITN use	0.36 (0.24, 0.54)	0.35 (0.23, 0.52)	0.35 (0.23, 0.52)
Pv infection	0.75 (0.58, 0.98)	0.77 (0.59, 1.01)	0.86 (0.63, 1.16)
Current fever		2.37 (1.76, 3.19)	3.08 (1.87, 5.06)
Pv infection × current fever			0.66 (0.36, 1.23)
Random effects	**Variance**	**variance**	**Variance**
Village	0.29	0.26	0.25
Child	0.40	0.40	0.40

Pv infection was associated with decreased odds of simultaneous *Pf* infection (Table 4.2, model 1 (OR 0.75 [0.58, 0.98])). This effect was diminished when fever was added to the model (Table 4.2, model 2 (OR 0.77 [0.59, 1.01])). A child with a fever had more than twice the odds of a concurrent *Pf* infection than when that same child did not have a fever (Table 4.2, model 2 (OR 2.37)). There was no significant interaction between *Pv* infection and fever, thus the effect of fever on *Pf* infections was independent of a child's *Pv* infection status (Table 4.2, model 3 (OR 0.66)).

A child's odds of having a *Pv* infection were lower when he/she had a concurrent *Pf* infection (Table 4.3, model 1 (OR 0.72) and model 2 (OR 0.74)). The main effect of fever was not significant (Table 4.3, model 2 (OR 0.84)); however, when stratified by *Pf* infection status, presence of fever and *Pf* infection indicated reduced odds of *Pv* infection (Table 4.3, model 3 (OR 0.38)).

The findings in Tables 4.2 and 4.3 might be due to several scenarios. First, it is possible that *Pf* infections with concurrent fever were suppressing *Pv* infections. Second, perhaps PCR methods were not able to detect very low levels of *Pv* infections in the presence of high density *Pf* infections where fevers were occurring. Furthermore, there could have been an innate immune response (i.e. non-species specific) to *Pf* infections that resulted in decreased *Pv* infections, especially when the body was battling a fever. Unfortunately, we cannot make the distinction between these explanations from these analyses.

Table 4.3: Odds ratio estimates (95% CI) from GLMMs for predicting binary *Pv* infections determined by PCR.

	Model 1 OR (95% CI)	**Model 2 OR (95% CI)**	**Model 3 OR (95% CI)**
Fixed effects			
Intercept	1.21 (0.65, 2.26)	1.26 (0.67, 2.35)	1.09 (0.58, 2.07)
Age	1.46 (1.17, 1.82)	1.46 (1.17, 1.81)	1.49 (1.20, 1.86)
Sin(week)	0.88 (0.74, 1.04)	0.88 (0.74, 1.04)	0.87 (0.73, 1.03)
Cos(week)	0.98 (0.83, 1.17)	0.99 (0.83, 1.18)	0.98 (0.82, 1.17)
ITN use	0.46 (0.30, 0.70)	0.46 (0.31, 0.70)	0.47 (0.31, 0.71)
Pf infection	0.72 (0.55, 0.94)	0.74 (0.56, 0.97)	0.92 (0.68, 1.25)
Current fever		0.85 (0.64, 1.14)	1.44 (0.93, 2.23)
Pf infection × current fever			0.38 (0.21, 0.68)
Random effects	**Variance**	**variance**	**Variance**
Village	0.14	0.14	0.15
Child	0.64	0.63	0.64

4.1.2 Estimating the effect of mixed infections on subsequent clinical episodes

Our objective in this section was to determine the effect of infection status at the start of an interval on clinical episode annualized rates. Using the binary infectious status variables described in the previous section, we fit GLMMs with *Pf* infection, *Pv* infection and the interaction between these two variables (measured at the start of an interval) predicting clinical episode annualized rates during the same interval. Results from fitting these models are summarized in Table 4.4 (*Pf* clinical episodes) and Table 4.5 (*Pv* clinical episodes).

Not surprisingly, *Pf* infection at the start of an interval was positively associated with experiencing clinical episodes caused by *Pf* parasites during the interval. A child's rate of *Pf* clinical episodes increased by approximately 20 percent when he/she was infected by *Pf* parasites at the start of the interval (Table 4.4, models 1 (IRR 1.23) and 2 (IRR 1.26)). Interestingly, *Pv* infection at the start of an interval resulted in an even stronger positive association with rates of *Pf* clinical episodes compared to having a *Pf* infection (Table 4.4, models 2 (IRR 1.44) and 4 (IRR 1.38)). The interaction between the two was not significant, which indicated that there was not a multiplicative effect of co-infection. Once Pf_{mol}FOI annualized rate was added to the model, *Pf* infection at the start of the interval was no longer significant (Table 4.4, model 4 (IRR 1.10)); however, *Pv* infection at the start of the interval was still a significant predictor of *Pf* clinical episodes during that same interval (Table 4.4, model 4 (IRR 1.38)).

Table 4.4: Incidence rate ratio estimates (95% CI) from GLMMs for clinical episode annualized rates caused by *Pf* parasites.

	Model 1 IRR (95% CI)	**Model 2 IRR (95% CI)**	**Model 3 IRR (95% CI)**	**Model 4 IRR (95% CI)**
Fixed effects				
Intercept	0.43 (0.14, 1.36)	0.35 (0.11, 1.11)	0.34 (0.11, 1.08)	0.26 (0.09, 0.75)
Age	2.99 (1.20, 7.44)	2.90 (1.17, 7.21)	2.85 (1.14, 7.08)	1.71 (0.73, 4.01)
Age^2	0.83 (0.70, 0.99)	0.83 (0.70, 1.00)	0.84 (0.70, 1.00)	0.90 (0.77, 1.07)
Sin(week)	0.95 (0.82, 1.09)	0.96 (0.84, 1.11)	0.96 (0.84, 1.10)	0.93 (0.81, 1.07)
Cos(week)	1.68 (1.48, 1.92)	1.68 (1.47, 1.91)	1.68 (1.47, 1.92)	1.27 (1.11, 1.46)
ITN use	0.62 (0.46, 0.83)	0.65 (0.49, 0.88)	0.66 (0.49, 0.88)	0.99 (0.77, 1.26)
Pf infection	1.23 (1.00, 1.51)	1.26 (1.03, 1.54)	1.41 (0.98, 2.04)	1.10 (0.90, 1.34)
Pv infection		1.44 (1.16, 1.78)	1.56 (1.15, 2.12)	1.38 (1.12, 1.69)
$Pf \times Pv$ infection			0.85 (0.56, 1.29)	
$(Pf_{mol}$FOI annualized rate$)^{1/3}$				2.09 (1.90, 2.28)
Random effects				
Village	0.05	0.05	0.05	0.01
Child	0.14	0.13	0.13	0.0

Table 4.5: Incidence rate ratio estimates (95% CI) from GLMMs for clinical episode annualized rates caused by *Pv* parasites.

	Model 1 **IRR (95% CI)**	**Model 2** **IRR (95% CI)**	**Model 3** **IRR (95% CI)**	**Model 4** **IRR (95% CI)**
Fixed effects				
Intercept	4.16 (2.35, 7.38)	4.17 (2.35, 7.42)	4.04 (2.26, 7.22)	0.93 (0.50, 1.74)
Age	0.53 (0.44, 0.65)	0.55 (0.45, 0.66)	0.54 (0.45, 0.66)	0.53 (0.44, 0.64)
Sin(week)	0.91 (0.78, 1.05)	0.93 (0.80, 1.07)	0.93 (0.80, 1.07)	0.98 (0.85, 1.14)
Cos(week)	1.44 (1.25, 1.67)	1.45 (1.25, 1.68)	1.46 (1.26, 1.69)	1.24 (1.06, 1.44)
ITN use	1.07 (0.71, 1.59)	1.04 (0.70, 1.55)	1.04 (0.70, 1.56)	1.35 (0.95, 1.93)
Pv infection	1.27 (1.01, 1.60)	1.28 (1.01, 1.61)	1.37 (1.05, 1.79)	1.19 (0.95, 1.50)
Pf infection		0.86 (0.67, 1.11)	0.99 (0.68, 1.46)	0.72 (0.56, 0.93)
Pv × *Pf* infection			0.79 (0.49, 1.28)	
$(Pv_{mol}$FOI annualized rate$)^{1/3}$				2.04 (1.84, 2.26)
Random effects				
Village	0.22	0.21	0.21	0.29
Child	0.55	0.55	0.55	0.27

Pv infection at the start of an eight weeks interval was associated with a 30 percent increase in the rate of clinical episodes caused by *Pv* parasites (Table 4.5, models 1 (IRR 1.27), and 2 (IRR 1.28)), but *Pf* infection was not (Table 4.5, model 2 (IRR 0.86)). There was no significant interaction between the two species of infections (Table 4.5, model 3 (IRR 0.79 [0.49, 1.28])). Once *Pv* $_{mol}$FOI was added to the model, *Pv* infection was no longer a significant predictor; however, *Pf* infection became significantly negatively associated with *Pv* clinical episodes (Table 4.5, model 4 (IRR 0.72 [0.56, 0.93])). Coefficients for age, ITN use, and seasonality were all similar to those estimated in Chapter 2 for both species.

The results in Tables 4.4 and 4.5 are limited by the fact that some children were treated during the interval. Thus, the infection status at the start of the interval was not relevant to any clinical episodes after the first episode. A better approach would be to determine the effect of infection status at the time of the clinical episode, but we do not have blood samples for the asymptomatic or healthy children during those episodes, so there would be no comparison group.

We ran one additional model to get an estimate of the effect of mixed infections on presence of fever. Again, we fit a binomial GLMM with all relevant covariates and random effects. The interaction term between *Pf* and *Pv* infection at the time of the fever was significantly negative (OR 0.46 (0.27, 0.80)), indicating that a child with a mixed infection had considerably lower odds of concurrent fever compared to when that same child did not have a mixed infection. However, a single species *Pf* infection was significantly predictive of concurrent fever in the same model (OR 3.82 (2.43, 5.99)). These results suggest that, when there was a mixed *Pf* and *Pv* infection, *Pv* might have been protective against fever, or the innate immune response to *Pf* could have been suppressing *Pv* below the limit of detection when a child was experiencing a fever. We also added a variable that accounted for the overall exposure during the cohort. This variable was the sum of unique *Pf* clones divided by the sum of the years-at-risk over the entire cohort for each child. This variable was not significant and did not change the effects of the other variables in the model. Therefore, it did not seem plausible that the relationship between mixed infections and fever was due to differences in exposure.

4.2 Discussion

The results presented in this chapter suggest that *Pv* infection at the start of an eight weeks interval was associated with an increase in a child's rate of *Pf* clinical episodes, even after accounting for *Pf* $_{mol}$FOI. Conversely, *Pf* infection was associated with a significantly lower rate of *Pv* clinical episodes. Fever was highly positively associated with *Pf* infection but was not associated with *Pv* infection. The proportion of infected children with fever was highest in those infected with single-species *Pf*. The estimated negative association between mixed infections and clinical episodes might have been due to the fact that many of the *Pf* single-species infections with concurrent fever had high *Pf* parasite density, thus making it difficult to detect the minority species, i.e. *Pv*. In other words, the failure of laboratory methods to detect a mixed infection when one species dominated the other could have had a big impact on the results in this study. Unfortunately, the analyses in this chapter do not warrant causal interpretations of the relationships between mixed infections and clinical episodes.

5 Conclusions

The findings from the PNG study presented in this dissertation have the potential to impact malaria research and prevention. The analyses presented in the first chapter suggested a strong positive relationship between the rates of acquisition of both *Pf* and *Pv* infections and the rates of homologous clinical episodes. *Pf* $_{mol}$FOI, in particular, would be a cheaper and simpler measure for estimating transmission intensity than current measures, such as entomological inoculation rate. Force of blood stage infection of *Pv* parasites was also a good measure of transmission intensity, but the magnitude of the measure should be interpreted with more caution due to the presence of relapsing clones. The third chapter provided evidence that rates of acquisition of *Pf* and *Pv* infections were significantly positively associated in children living in a rural area of PNG. To our knowledge, a bivariate analysis of these two measures is the first of its kind. However, the BPLM only provided an estimate of association between the two rates of infections and did not provide any knowledge about the effect of mixed infections on clinical symptoms of malaria. The results presented in Chapter 4 suggested that, at the time of a blood sample, a child with a mixed infection had lower odds of having a fever than when that same child did not have a mixed infection. Furthermore, because a child with a single-species *Pf* infection had much higher odds of concurrent fever, then it is possible that the presence of *Pv* parasites inhibited fever in children with mixed infections. Alternatively, the culprit might have been increased exposure to clones of both species and a subsequent immune response that was not species-specific. Furthermore, as we stated in the Chapter 4 discussion, there is always the possibility of missing clones using either LM or PCR, so the minority infection with respect to parasite density could have been missed, resulting in mixed infections being misclassified as single-species.

The epidemiological findings from the analyses presented in this dissertation contribute to the knowledge of the complex interactions between the environment, host, pathogen, and vector of parasites that cause malaria. The use of longitudinal random effects models to estimate the relationships between the predictors and outcomes permitted the inclusion of important covariates and covariance structures that typical linear models do not. Furthermore, the use of a bivariate model to estimate the association between rates of acquisition of heterologous infections allowed for the inclusion of important covariates that influenced these measures. However, the results of the simulation study and model diagnostics both highlighted the importance of checking the fit of the model to the data before drawing firm conclusions.

The data described in this dissertation were from a relatively small cohort of children living in a rural area of PNG. To make more generalizable statements about the interactions between the two species of malaria parasites, it would be important to apply these same statistical models to larger data sets and from different areas of endemic *Pf* and *Pv* transmission.

Bibliography

Aitchison, J. and C. Ho (1989). The multivariate Poisson-log normal distribution. *Biometrika 76*(4), 643–653.

Alonso, P., J. Sacarlal, J. Aponte, A. Leach, et al. (2004). Efficacy of the RTS,S/AS02A vaccine against *Plasmodium falciparum* infection and disease in young African children: randomised controlled trial. *Lancet 364*(9443), 1411–1420.

Backus, L., D. Boothroyd, and L. Deyton (2005). HIV, hepatitis C and HIV/hepatitis C virus co-infection in vulnerable populations. *AIDS 19*(suppl 3), S13–S19.

Bates, D., M. Maechler, and B. Bolker (2012). *lme4: Linear mixed-effects models using S4 classes*. R package version 0.999999-0.

Bejon, P., T. Williams, A. Liljander, A. Noor, et al. (2010). Stable and unstable malaria hotspots in longitudinal cohort studies in Kenya. *PLoS Med 7*(7), e1000304.

Bretscher, M., F. Valsangiacomo, S. Owusu-Agyei, M. Penny, I. Felger, and T. Smith (2010). Detectability of *Plasmodium falciparum* clones. *Malar J 9*(234).

Burkot, T., P. Graves, R. Paru, R. Wirtz, and P. Heywood (1988). Human malaria transmission studies in the *Anopheles punctulatus* complex in Papua New Guinea: sporozoite rates, inoculation rates, and sporozoite densities. *Am J Trop Med Hyg 39*(2), 135–144.

Cattani, J., J. Moir, F. Gibson, M. Ginny, et al. (1986). Small-area variations in the epidemiology of malaria in Madang Province. *PNG Med J 29*(1), 11–17.

Charlwood, J., P. Graves, and M. Alpers (1986). The ecology of the *Anopheles punctulatus* group of mosquitoes from Papua New Guinea: a review of recent work. *P N G Med J* (1), 19–26.

Ciuca, M., L. Ballif, and M. Chelarescu-Vieru (1934). Immunity in malaria. *Trans Royal Soc Trop Med Hyg 27*(4).

Coovadia, H. and P. Wilkinson (1998). Childhood human immunodeficiency virus and tuberculosis co-infections: reconciling conflicting data. *Int J Tuberc Lung Dis 2*(10), 844–851.

Diggle, P., P. Heagerty, K.-Y. Liang, and S. Zeger (2002). *Analysis of Longitudinal Data* (2 ed.). New York, NY: Oxford University Press.

Doolan, D., C. Dobano, and J. Baird (2009). Acquired immunity to malaria. *Clin Microbiol Rev 22*, 13–36.

Dye, C. (1992). The analysis of parasite transmission by bloodsucking insects. *Annu Rev Entomol 37*, 1–19.

Falk, N., N. Maire, W. Sama, S. Owusu-Agyei, et al. (2006). Comparison of PCR-RFLP and Genescan-based genotyping for analyzing infection dynamics of *Plasmodium falciparum*. *Am J Trop Med Hyg 74*(6), 944–950.

Gunewardena, D., R. Carter, and K. Mendis (1994). Patterns of acquired anti-malarial immunity in Sri Lanka. *Mem Inst Oswaldo Cruz 89*(Suppl 2), 63–65.

Hadfield, J. D. (2010). MCMC methods for multi-response generalized linear mixed models: The MCMCglmm R package. *Journal of Statistical Software 33*(2), 1–22.

Haenszel, W., D. Loveland, and M. Sirken (1962). Lung-cancer mortality as related to residence and smoking histories. I. White males. *J Natl Cancer Inst 28*(4), 947–1001.

Hay, S., D. Rogers, J. Toomer, and R. Snow (2000). Annual *Plasmodium falciparum* entomological inoculation rates (EIR) across Africa: literature survey, internet access and review. *Trans R Soc Trop Med Hyg 94*(2), 113–127.

Hii, J., T. Smith, A. Mai, S. Mellor, et al. (1997). Spatial and temporal variation in abundance of *Anopheles* (*Diptera:Culicidae*) in a malaria endemic area in Papua New Guinea. *J Med Entomol 34*(2), 193–205.

Imwong, M., G. Snounou, S. Pukrittayakamee, N. Tanomsing, J. Kim, et al. (2007). Relapses of *Plasmodium vivax* infection usually result from activation of heterologous hypnozoites. *J Infect Dis 195*, 927–933.

Jeffery, G. (1966). Epidemiological significance of repeated infections with homologous and heterologous strains and species of *Plasmodium*. *Bull World Health Organ 35*, 873–882.

Kasehagen, L., I. Mueller, D. McNamara, M. Bockarie, B. Kiniboro, et al. (2006). Changing patterns of *Plasmodium* blood-stage infections in the Wosera region of Papua New Guinea monitored by light microscopy and high throughput PCR diagnosis. *Am J Trop Med Hyg 75*, 588–596.

Koch, R. (1900). Dritter bericht ber die tŁtigkeit der malaria expedition. *Deutsche Medizinische Wochenschrift 17*.

Koepfli, C., A. Ross, B. Kiniboro, T. Smith, P. Zimmerman, et al. (2011). Multiplicity and diversity of *Plasmodium vivax* infections in a highly endemic region in Papua New Guinea. *PLoS Negl Trop Dis 5*, e1424.

Koepfli, C., S. Schoepflin, M. Bretscher, E. Lin, et al. (2011). How much remains undetected? Probability of molecular detection of human *Plasmodia* in the field. *PLoS ONE 6*(4), e19010.

Langhorne, J., F. Ndungu, A. Sponaas, and K. Marsh (2008). Immunity to malaria: more questions than answers. *Nat Immunol 9*, 725–732.

Lengeler, C. (2004). Insecticide-treated bed nets and curtains for preventing malaria. *Cochrane Database Syst Rev 2*, CD000363.

Lin, E., B. Kiniboro, L. Gray, S. Dobbie, L. Robinson, et al. (2010). Differential patterns of infection and disease with *P. falciparum* and *P. vivax* in young Papua New Guinean children. *PLoS ONE 5*(2), e9047.

Macdonald, G. (1950). The analysis of malaria parasite rates in infants. *Tropical Diseases Bulletin 47*, 915–938.

Maitland, K., T. Williams, S. Bennett, C. Newbold, T. Peto, et al. (1996). The interaction between *Plasmodium falciparum* and *P. vivax* in children on Espiritu Santo Island, Vanuatu. *Trans R Soc Trop Med Hyg 90*, 614–620.

Maurer, A. and D. Sturchler (2000). A waterborne outbreak of small round structured virus, campylobacter and shigella co-infections in La Neuveville, Switerland, 1998. *Epidemiol Infect 125*, 325–332.

Mayxay, M., S. Pukrittayakamee, P. Newton, and N. White (2004). Mixed-species malaria infections in humans. *Trends in Parasitol 20*(5), 233–240.

McCullagh, P. and J. Nelder (1989). *Generalized Linear Models* (2 ed.). Boca Raton, FL: Chapman & Hall/CRC.

McCulloch, C. (2008). Joint modeling of mixed outcome types using latent variables. *Stat Methods Med Res 17*, 53–73.

McKenzie, F., D. Smith, W. O'Meara, J. Forney, A. Magill, et al. (2006). Fever in patients with mixed-species malaria. *Clin Infect Dis 42*, 1713–1718.

Michon, P., J. Cole-Tobian, E. Dabod, S. Schoepflin, J. Igu, et al. (2007). The risk of malarial infections and disease in Papua New Guinean children. *Am J Trop Med Hyg 76*, 997–1008.

Msuya, F. and C. Curtis (1991). Trial of pyrethroid impregnated bednets in an area of Tanzania holoendemic for malaria. part 4. effects on incidence of malaria infection. *Acta Trop 49*(3), 165–171.

Mueller, I., S. Schoepflin, T. Smith, K. Benton, M. Bretscher, et al. (2012). Force of infection is key to understanding the epidemiology of *Plasmodium falciparum* malaria in Papua New Guinean children. *Proc Natl Acad Sci U S A 109*(25), 10030–10035.

Mueller, I., S. Widmer, D. Michel, S. Maraga, D. McNamara, et al. (2009). High sensitivity detection of *Plasmodium* species reveals positive correlations between infections of different species, shifts in age distribution and reduced local variation in Papua New Guinea. *Malar J 8*(41).

Phimpraphi, W., R. Paul, S. Yimsamran, S. Puangsa-art, N. Thanyavanich, et al. (2008). Longitudinal study of *Plasmodium falciparum* and *Plasmodium vivax* in a Karen population in Thailand. *Malar J 7*(99).

Pinheiro, J. and D. Bates (1995). Approximations to the log-likelihood function in the nonlinear mixed-effects model. *J Comp Graph Stat 4*(1), 12–35.

Port, G., P. Boreham, and J. Bryan (1980). The relationship of host size to feeding by mosquitoes of the *Anopheles-gambiae* giles complex (*Diptera, Culicidae*). *Bull Entomol Res 70*(1), 133–144.

Preston, F. (1948). The commonness, and rarity, of species. *Ecology 29*(3), 254–283.

R Core Team (2013). *R: A Language and Environment for Statistical Computing*. Vienna, Austria: R Foundation for Statistical Computing.

Sama, W., S. Owusu-Agyei, I. Felger, K. Dietz, and T. Smith (2006). Age and seasonal variation in the transition rates and detectability of *Plasmodium falciparum* malaria. *Parasitology 132*(Part 1), 13–21.

Sama, W., S. Owusu-Agyei, I. Felger, P. Vounatsou, and T. Smith (2005). An immigration-death model to estimate the duration of malaria infection when detectability of the parasite is imperfect. *Stat Med 24*(21), 3269–3288.

SAS Institute (2013). *Copyright 2013 SAS Institute Inc. SAS and all other SAS Institute Inc. product or service names are registered trademarks or trademarks of SAS Institute Inc., Cary, NC, USA.* Cary, NC, USA.

Schoepflin, S., F. Valsangiacomo, E. Lin, B. Kiniboro, I. Mueller, and I. Felger (2009). Comparison of *Plasmodium falciparum* allelic frequency distribution in different endemic settings by high-resolution genotyping. *Malar J 8*(250).

Smith, T., I. Felger, N. Fraser-Hurt, and H. Beck (1999). Effect of insecticide-treated bed nets on the dynamics of multiple *Plasmodium falciparum* infections. *Trans R Soc Trop Med Hyg 93*(Suppl 1), 53–57.

Smith, T., I. Felger, M. Tanner, and H. Beck (1999). Premunition in *Plasmodium falciparum* infection: insights from the epidemiology of multiple infections. *Trans R Soc Trop Med Hyg 93*(Suppl 1), 59–64.

Smith, T., B. Genton, K. Baea, N. Gibson, A. Narara, et al. (2001). Prospective risk of morbidity in relation to malaria infection in an area of high endemicity of multiple species of *Plasmodium*. *Am J Trop Med Hyg 64*(5,6), 262–267.

Smith, T., N. Maire, K. Dietz, G. Killeen, et al. (2006). Relationship between the entomologic inoculation rate and the force of infection for *Plasmodium falciparum* malaria. *Am J Trop Med Hyg 75*(2 Suppl), 11–18.

Smith, T. and P. Vounatsou (2003). Estimation of infection and recovery rates for highly polymorphic parasites when detectability is imperfect using hidden Markov models. *Stat Med 22*(10), 1709–1724.

Snounou, G. and N. White (2004). The co-existence of *Plasmodium*: sidelights from falciparum and vivax malaria in Thailand. *Trends in Parasitol 20*(7), 333–339.

Snow, R., J. Omumbo, B. Lowe, C. Molyneux, J. Obiero, et al. (1997). Relation between severe malaria morbidity in children and level of *Plasmodium falciparum* transmission in Africa. *Lancet 349*, 1650–1654.

White, N. (2011). Determinants of relapse periodicity in *Plasmodium vivax* malaria. *Malar J 10*(297).

Woolhouse, M., C. Dye, J. Etard, T. Smith, et al. (1997). Heterogeneities in the transmission of infectious agents: implications for the design of control programs. *Proc Natl Acad Sci U S A 94*(1), 338–342.

Appendices

Figure A1. Diagnostic plots of residuals for marginal predicted values of clinical episodes by interval.

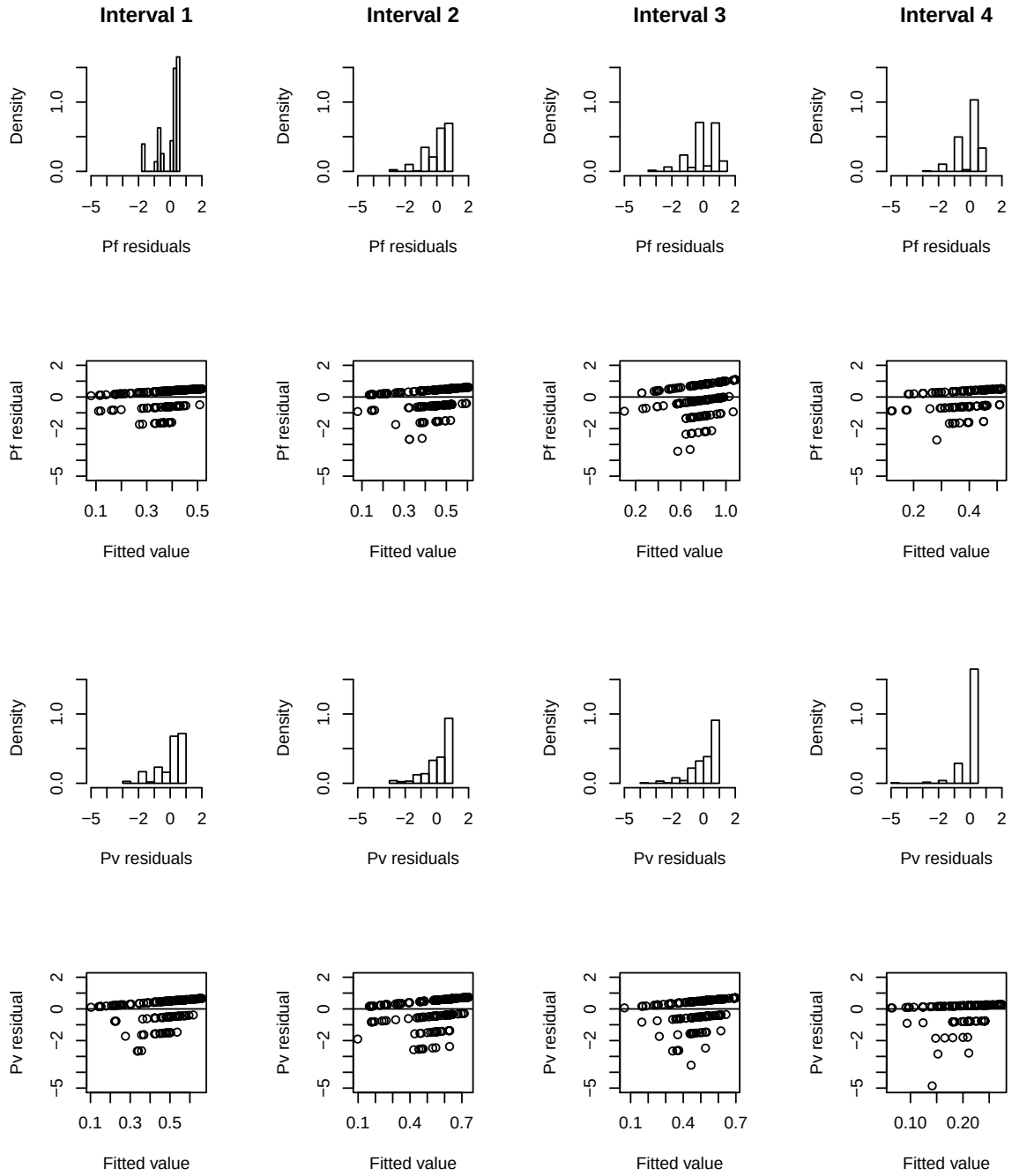

Figure A2. Distributions of parameter estimates from BPLMs fit to 1,000 random samples of 90 percent of the PNG data. (All values multiplied by 100).